

Persistence of a reef fish metapopulation via network connectivity: theory and data

Allison G. Dedrick^{a,*1}

Katrina A. Catalano^a

Michelle R. Stuart^a

J. Wilson White^b

Humberto Montes, Jr.^c

Malin Pinsky^a

a. Department of Ecology Evolution and Natural Resources, Rutgers University, 14 College Farm Road, New Brunswick, NJ 08901 USA;

b. Department of Fisheries and Wildlife, Coastal Oregon Marine Experiment Station, Oregon State University, Newport, OR 97365 USA;

c. Visayas State University, Pangasugan, Baybay City, 6521 Leyte, Philippines

* Corresponding author; e-mail: agdedrick@gmail.com

1. Current address: Stanford Woods Institute for the Environment, Stanford University, Stanford, CA 94305 USA.

Running title: (45 characters including spaces) Empirical metapopulation persistence

Keywords: metapopulation dynamics, self-persistence, network persistence, *Amphiprion clarkii*, connectivity (5/10)

Type of article: Letters

Statement of authorship: MLP, JWW, and AGD conceived of and designed the study. MLP, MRS, KAC, and AGD conducted field work, collected data, and considered data use and interpretation. HRM facilitated field work and provided local ecosystem context and knowledge. AGD analysed the data and wrote the first draft of the manuscript. All authors contributed substantially to revisions.

Data accessibility statement: Sample data, metadata, GIS data, and analysis code is stored in a GitHub repository and will be made public after acceptance. The repository will be archived with a DOI through Zenodo.

Words in the abstract: 129/150

Words in the main text: about 5500

Number of references: 62

Number of main figures, tables, and text boxes: 6

Number of supplementary figures, tables, and text boxes: 19

Acknowledgements

We thank Visayas State University for providing scientific and logistical support during our field sampling in Leyte, Philippines, as well as the municipalities of Bay Bay City and Albuera. We particularly thank Geralde Sucano, Jennifer Hoey, Patrick Flanagan, Joyce Ong, Apollo Lizano, Cecil Bantiles, Rodney Silvado, Beverlito Montalban, Teresita Idara, Rogello Nicanor, Liza Espinosa, Shem San Jose, Noel Alquino, Carlos Balansuna, Froilan Beas, Danilo Marine, Tony Nahacky, and Arturo Bastasa. For financial support, we thank Rutgers School of Environmental and Biological Sciences, NSF #OCE-1430218, an Alfred P. Sloan Research Fellowship, and an ORAU Ralph E. Powe Junior Faculty Enhancement award. This is publication number ## of PISCO, the Partnership for Interdisciplinary Study of Coastal Oceans, funded primarily by the David and Lucile Packard Foundation.

Abstract

Determining whether a metapopulation can persist requires an understanding of both demographic parameters and connectivity among patches. This is well understood in theory but has proved challenging to test empirically. We assessed persistence for

a network of patches along a coastline in a metapopulation of yellowtail anemonefish (*Amphiprion clarkii*) using seven years of annual sampling data. We found that this metapopulation produced enough surviving offspring to replace itself but that the spatial pattern of connectivity made it unlikely to persist in isolation despite stable abundances through time. To persist, the metapopulation would need higher fecundity or would need to retain essentially all of the recruits it produced. This first assessment of persistence in a marine metapopulation shows that stable abundance alone is not an indicator of persistence, emphasizing the necessity of untangling demographic and connectivity processes to understand metapopulation dynamics.

(130/150 words)

Introduction (622 words)

The dynamics and persistence of metapopulations depend both on connectivity
3 among patches and on demographic rates within each patch (Hastings and Botsford, 2006; Hanski, 1998). For marine species, connectivity among habitat patches primarily occurs during planktonic larval stages when individuals are hard to track
6 and are able to travel long distances with ocean currents. Because larval connectivity has been perceived to be the greatest uncertainty in these systems, research has centered on quantifying that component (reviewed by White et al., 2019). More
9 recently, it has become apparent that variation in demographic rates among patches is an equally uncertain aspect of marine metapopulation dynamics (Hameed et al., 2016; White and Samhouri, 2011). Given both of those uncertainties, and driven
12 by both fundamental ecological questions and applied needs (Botsford et al., 2001;

White et al., 2010), a large body of theory has developed to describe how connectivity and local demography interact to determine whether marine metapopulations
15 persist (Burgess et al., 2014; Botsford et al., 2019). Testing this theory, however, has proven substantially more difficult.

For any population to persist, individuals must on average replace themselves
18 during their lifetime. Assessing replacement must account for demographic processes across the life cycle, including how likely individuals are to survive to the next age or stage, their expected fecundity at each stage, and the survival to recruitment of
21 any offspring produced. In a spatially structured population, how the offspring are distributed across space is also important (Hastings and Botsford, 2006).

A metapopulation can persist via two mechanisms: 1) at least one patch achieves
24 replacement in isolation, or 2) multiple patches receive enough recruitment to achieve replacement through multi-generational loops of connectivity with other patches in the metapopulation (Hastings and Botsford, 2006; Burgess et al., 2014). In the first
27 case (termed self-persistence), enough of the offspring produced at one patch are retained there for it to persist. In the second case (network persistence), closed loops of connectivity among patches - in which offspring from one patch recruit to another
30 patch but eventually send offspring back to the first in a future generation - provide the patches with enough recruitment to persist within the network. Theory predicts that habitat patches that are large relative to the mean dispersal distance are likely
33 to be self-persistent (White et al., 2010).

New ways of identifying individuals and determining their origins now allow better measurements of connectivity in marine populations (Almany et al., 2017; D'Aloia

³⁶ et al., 2013). Additionally, a better appreciation of the relevant population dynamic theory has led to measurement of the appropriate demographic factors necessary to assess persistence in field metapopulations (Carson et al., 2011; Hameed et al.,
³⁹ 2016; Johnson et al., 2018; Salles et al., 2015). To date, research has suggested that populations on isolated islands can be self-persistent, which might be expected given that they lack nearby populations from which to receive larvae and would go locally
⁴² extinct if they did not achieve replacement (Salles et al., 2015). In contrast, small habitat patches spread across a larger reef metapopulation appear to rely on input from surrounding and intervening patches for persistence (Johnson et al., 2018).
⁴⁵ Persistence has yet to be quantified in the field for an entire continuous marine metapopulation, however, such as all of the patches along a coastline.

Here, we further our understanding of metapopulation dynamics in a network
⁴⁸ of patches along a coastline through a study of yellowtail anemonefish (*Amphiprion clarkii*) in the Philippines. We assessed persistence for all patches of habitat within a metapopulation spread across 30 km of coastline. Based on seven years of data,
⁵¹ we found that, despite containing multiple patches with large abundances that were stable over time, the metapopulation was not likely to be persistent and required immigration from outside patches to persist.

⁵⁴ **Methods**

Persistence theory and metrics

We considered four primary metrics to assess whether and how the anemonefish metapopulation was persistent: 1) lifetime recruit production (LRP) to assess whether the metapopulation had enough offspring that survived anywhere to achieve replacement, 2) self-persistence (SP) to assess whether any individual patch could persist in isolation without input from other patches, 3) network persistence (λ_c) to assess whether the metapopulation was persistent as a connected unit, and 4) local replacement (LR) to assess whether a sufficient number of recruits were retained anywhere within the metapopulation to achieve replacement, without explicitly estimating dispersal. We explain each metric below in detail. To represent the uncertainty in our estimates, we calculated each metric 1000 times, sampling each input parameter from a distribution representing the uncertainty in the empirical estimate (details in SI A.9). In our results, we show best estimates of each metric along with uncertainty bounds, defined as the middle 95% of the distribution of values calculated in this Monte Carlo procedure.

Lifetime recruit production (LRP)

LRP_{*i*} is the expected number of recruits a recruit on patch *i* will produce in its lifetime,

$$\text{LRP}_i = \text{LEP}_i \times S_e, \quad (1)$$

where LEP_i (lifetime egg production) is the patch-specific number of eggs a recruit produces in its lifetime and S_e (egg-recruit survival) is the fraction of eggs that survive to become recruits (Fig. D.1).

If $\text{LRP} \geq 1$, individuals produced enough surviving offspring, before considering dispersal, to potentially achieve replacement. If $\text{LRP} < 1$, the population could not persist without input from outside patches. We considered all recruits produced by adults in our metapopulation to estimate LRP_i , regardless of where they settled.

Self-persistence (SP)

SP_i is the number of offspring a recruit produces that survive to become recruits and settle in the natal patch,

$$\text{SP}_i = \text{LRP}_i \times p_{i,i}, \quad (2)$$

where $p_{i,i}$ is the probability of larval retention on patch i .

A patch i is self-persistent if $\text{SP}_i \geq 1$. If at least one patch is self-persistent, the metapopulation as a whole persists as well (Hastings and Botsford, 2006; Burgess et al., 2014).

⁸⁷ **Network persistence (λ_c)**

Network persistence is the largest real eigenvalue λ_C of the realized connectivity matrix C ,

$$C_{i,j} = \text{LRP}_i \times p_{i,j}, \quad (3)$$

⁹⁰ created by multiplying lifetime recruit production (LRP_i) by dispersal probabilities among pairs of patches ($p_{i,j}$) (Burgess et al., 2014). The diagonal entries of C are the self-persistence values for each patch (SP_i).

⁹³ Network persistence explicitly considers dispersal of individuals among patches in addition to the reproduction and survival at each patch and requires $\lambda_C \geq 1$ for the network to persist without outside input (Hastings and Botsford, 2006; White
⁹⁶ et al., 2010; Burgess et al., 2014).

Local replacement (LR)

Local replacement (LR) is the number of recruits a recruit produces in its lifetime
⁹⁹ that return to settle within the focal metapopulation. LR is related to LRP, but in contrast, LRP also includes recruits that settle outside of the focal metapopulation.
LR is defined as

$$\text{LR} = \text{LEP}_* \times R_e, \quad (4)$$

¹⁰² where LEP_* is lifetime egg production averaged across patches and R_e is the

proportion of eggs that survived and returned to recruit at the patches in our focal metapopulation (the 30 km section of coastline). R_e is a modification of egg-recruit survival (S_e) that implicitly includes dispersal.

If $LR \geq 1$, enough offspring were locally retained to achieve replacement if they were evenly spread among patches, but the actual dispersal patterns among the metapopulation patches may still prevent replacement if the pattern of multigenerational replacement does not satisfy the Hastings and Botsford (2006) criterion. LR and λ_c both assess the ability of our patches to persist as an isolated group, but LR treats the network as one large homogenous patch while λ_c explicitly accounts for the structure and connectivity among patches.

Study species

We focused on a tropical metapopulation of yellowtail anemonefish (*Amphiprion clarkii*, Fig. 2c). Yellowtail anemonefish have a mutualistic relationship with anemones that house small colonies of fish (Buston, 2003b; Fautin et al., 1992). Yellowtail anemonefish are protandrous hermaphrodites and maintain a size-structured hierarchy; within an anemone, the largest fish is the breeding female, the next largest is the breeding male, and any smaller fish are non-breeding juveniles. The fish move up in rank to become breeders only after the larger fish have died. In the tropical patch reef habitat of the Philippines, yellowtail anemonefish primarily spawn from November to May and lay clutches of benthic eggs that the parents protect and tend (Ochi, 1989; Holtswarth et al., 2017). Larvae hatch after about six days and spend 7-10 days in the water column before returning to reef habitat to settle in an

anemone (Fautin et al., 1992).

¹²⁶ Anemonefish are well-suited to metapopulation studies because dispersal only occurs during the larval phase and adults have limited movement on discrete habitat patches (anemones) (e.g., Buston and DAloia, 2013; Salles et al., 2015; Almany et al.,
¹²⁹ 2017). Yellowtail anemonefish tend to behave more like other reef fishes, with wider-ranging territories and stronger swimming abilities (Hattori and Yanagisawa, 1991; Ochi, 1989) than the smaller *A. percula* commonly used in metapopulation studies
¹³² (e.g., Buston et al., 2011; Salles et al., 2015).

Field data collection

We focused on a set of nineteen reef patches spanning 30 km along the western coast
¹³⁵ of Leyte island facing the Camotes Sea in the Philippines (Fig. 2a). The habitat patches covered approximately 20% of the sampling region and consisted of rocky patches of coral reef separated by sand flats (Fig. 2a,b). To the north, the patches
¹³⁸ were isolated from nearby habitat with no substantial reef habitat for at least 20 km, a distance greater than the mean dispersal distance for this species (Pinsky et al., 2010). As such, we considered this to be a relatively isolated metapopulation.
¹⁴¹ Located near a populated coastline, the region experiences anthropogenic effects including fishing, pollution, and runoff from agriculture and a nearby riverbed gravel mine, as well as reef-destroying storms like Haiyan and other typhoons in 2013.

¹⁴⁴ From 2012-2018, we sampled fish and habitat at most patches each year (Table A4). Divers using SCUBA and tethered to GPS readers swam the extent of each patch and visited anemones inhabited by yellowtail anemonefish. At each anemone,

¹⁴⁷ the divers caught fish 3.5 cm and larger, took a tissue sample, measured fork length,
and noted tail color as an indicator of life stage. Starting in 2015, fish 6.0 cm
¹⁵⁰ and larger were also tagged with a passive integrated transponder (PIT) tag unless
already tagged. Divers also looked for eggs around each anemone and measured and
photographed any clutches found. In total, we took fin clips from and genotyped
2406 fish and PIT-tagged 1929 fish across all years and patches combined, marking
¹⁵³ 3053 individual fish.

Estimating demographic and dispersal parameters from empirical data

¹⁵⁶ Parentage analysis and dispersal kernel

Over seven years of sampling, we genotyped 1729 potential parents and 791 juveniles at 1340 single nucleotide polymorphisms (SNPs) and found 71 parent-offspring matches (Catalano et al., in prep). We used a distance-based dispersal kernel fit from the parent-offspring matches (Catalano et al., in prep; Bode et al., 2018), where the relative probability of dispersal $p(d)$ is a function of distance d in kilometers and parameters θ and $z = e^{K_d}$ that control the shape and scale of the kernel (Fig. 3a, Table A1, uncertainty details in SI A.9.0.1). The dispersal kernel estimates the relative dispersal by distance for fish that have survived and recruited so does not separately estimate pre-settlement mortality. To find the probability of fish dispersing among our patches, we numerically integrated the dispersal kernel using the distance from the middle of the origin patch (i) to the closest (d_1) and farthest (d_2) edges of the

¹⁶⁸ destination patch (j), with distances calculated using the `geosphere` package in R
 (Hijmans, 2017):

$$p_{i,j} = \frac{z\theta}{2\gamma(\frac{1}{\theta})} \int_{d_1}^{d_2} ze^{-(zd)^\theta} dd. \quad (5)$$

Growth and survival: mark-recapture analyses

¹⁷¹ Fish marked through geneotyping and PIT tags allowed us to estimate growth and survival through mark-recapture. In total, we had 3053 marked fish with size and stage data at each capture.

¹⁷⁴ For growth, we used a von Bertalanffy growth curve:

$$\begin{aligned} L_{t+1} &= L_t + (L_\infty - L_t)[1 - e^{(-k)}] \\ &= e^{(-k)}L_t + L_\infty[1 - e^{(-k)}], \end{aligned} \quad (6)$$

¹⁷⁷ where L_∞ is the asymptotic maximum size across the metapopulation and k is the growth rate. We estimated the parameters from the slope m and y-intercept b of the relationship between the length at first capture L_t and the length at a later capture date L_{t+1} for fish recaptured after a year (within 345 to 385 days). The von Bertalanffy parameters are $k = -\ln(m)$ and $L_\infty = b(1 - m)$ (Hart and Chute, 2009) (Fig. 3b, Table A1, uncertainty details in SI A.9.0.2).

We used the full set of marked fish to estimate annual survival ϕ and probability of recapture p_r using the mark-recapture program MARK implemented in R through

₁₈₃ the package **RMark** (Laake, 2013). We fit several models with year, size, and patch effects on the probability of survival on a log-odds scale and selected the model with the lowest AIC_c (Fig. 3c, details in SI A.3, uncertainty details in SI A.9.0.3, and full list of models in Table A3).

Fecundity

₁₈₉ From a regression of eggs per clutch on female size and egg age (determined by the presence of eyed eggs), we found that fecundity increased with size (eqn. A.1, see details in SI A.4). We only considered reproductive effort for fish in the female stage and used the average size of first female observation for recaptured fish as the ₁₉₂ transition size L_f (Fig. 3d, uncertainty details in SI A.9.0.4).

Lifetime egg production (LEP)

We used an integral projection model (IPM) (Ellner et al., 2016) with size as the ₁₉₅ continuous structuring trait L to estimate lifetime egg production on each patch i (LEP_i). We initialized the IPM with one recruit-sized individual (recruit defined in SI A.1) at the initial annual time step ($t = 0$), then projected forward for 100 years. ₁₉₈ We used the size-dependent survival (eqn. B.1) and growth (eqn. 6) functions as the probability density functions in the kernel to project the individual into the next time step. The size distribution (v_L) at each time step represents the probability ₂₀₁ that the individual has survived and grown into each of the possible size categories, ranging from a minimum of $L_s = 0$ cm to a maximum of $U_s = 15$ cm divided into 100 equal size bins.

204 We then multiplied the size-distribution v_L at each time by the size-dependent fecundity f (eqn. A.1) to get the total number of eggs produced at each time step. Integrating across time and size gave the total number of eggs one recruit produced 207 in its lifetime (details in A.5, uncertainty details in SI A.9.0.7):

$$\text{LEP} = \int_{t=0}^{\infty} \int_{L=L_s}^{L=U_s} v_{L,t} f_L dL dt. \quad (7)$$

210 We calculated LEP by patch (LEP_i) and averaged across patches (LEP_*) for a fish of recruit size. We also calculated LEP for a fish of parent size (6.0 cm) averaged across patches (LEP_p), used below to estimate egg-recruit survival.

Accounting for density dependence

213 We would ideally assess persistence metrics when the population is at low abundance and not limited by density dependence because persistence is defined as having positive population growth at low density; at high density the population growth rate will slow to zero. Density dependence is particularly clear in anemonefish, which 216 have strong social hierarchies. Juveniles on an anemone will prevent others from settling there as well (seen in *A. percula*, Buston, 2003a). Each anemone, therefore, can house only one recently settled anemonefish. This density-dependent mortality 219 artificially reduces the apparent survival of new recruits (recruit defined in SI A.1), likely biasing persistence metrics. We accounted for this effect by scaling up our estimate of recruits (the numerator of eqn. 8, described next) by the proportional increase (DD) in unoccupied anemones if all of the anemones occupied by 222

yellowtail anemonefish were unoccupied, where p_A is the proportion of anemones occupied by yellowtail anemonefish and p_U is the proportion of unoccupied anemones:
 225 $DD = \frac{(p_U + p_A)}{p_U}$. We present results with this density dependence modification in the main text and without in the appendix (with subscript DD, Figs. D.9, D.10).

Survival from egg to recruit (S_e)

228 We estimated survival from egg to recruit (S_e) using parentage matches to find the number of surviving recruits produced by genotyped parents (similar to Johnson et al., 2018). However, the number of offspring we assigned back to parents (R_m) is
 231 a severe underestimate of the offspring produced by genotyped parents because we could not sample exhaustively. To account for offspring missed by our sampling, we divided R_m by four factors (described below and with details in SI A.8 and diagram
 234 Fig. D.2), in addition to multiplying by DD as described above, then divided by the number of eggs produced by genotyped parents:

$$S_e = \frac{\frac{DDR_m}{P_h P_c P_d P_s}}{N_g \text{LEP}_p}, \quad (8)$$

237 where N_g was the number of genotyped parents and LEP_p was the expected lifetime egg production for a fish that has already survived to parent size p (=6.0cm). LEP_p therefore does not include survival from recruit to parent sizes. P_h was the cumulative proportion of habitat in our patches that we sampled over time (details
 240 in SI A.8.0.1), P_c was the probability of capturing a fish if we sampled its anemone (details in SI A.8.0.2), P_d was the proportion of the total dispersal kernel area from

each of our patches covered by our sampling region (details in SI A.8.0.3), and P_s
243 was the proportion of suitable habitat in our sampling region (details in SI A.8.0.4).

To estimate the survival and retention of recruits back to our patches (needed for local replacement, LR, eqn. 4), we scaled only by P_h and P_c :

$$R_e = \frac{\frac{DDR_m}{P_h P_c}}{N_g \text{LEP}_p}. \quad (9)$$

246 Estimated abundance over time

We examined trends in abundance of breeding females at each patch over time ($F_{i,t}$)
to compare to our replacement-based persistence estimates. As with offspring, we
249 scaled up the number of females caught ($F_{c_{i,t}}$) at each patch i in each sampling year
 t by the proportion of habitat sampled in that patch and year ($P_{h_{i,t}}$) and by the
probability of capturing a fish P_c :

$$F_{i,t} = \frac{F_{c_{i,t}}}{P_{h_{i,t}} P_c} \quad (10)$$

252 We fit a mixed effects model to estimate the number of fish in each year as a
Poisson-distributed variable λ_a with random effects by patch for both intercept and
slope through time using the package `lme4` in R (Bates et al., 2015).

255 Exploring alternative geographies and larval navigation

Finally, we tested the sensitivity of metapopulation persistence to patch width and
to the proportion of the region that is habitat to understand whether the results

²⁵⁸ would likely be similar in other geographies. We varied the proportion of habitat
and the overall width of the region using 19 equally sized and spaced patches. We
created connectivity matrices using the new distances between patches and otherwise
²⁶¹ used the original parameter values and uncertainty sets, using adult survival from
the patch with median survival (the Elementary School patch) for all patches.

We also tested sensitivity to the ability of larvae to navigate to habitat by adding
²⁶⁴ up to a 1km buffer to the edges of the destination patches when integrating the
dispersal kernel and adjusting the scaling parameter P_s (eqn. 8) to account for fewer
larvae being lost between patches (details in SI A.7.0.1).

²⁶⁷ **Results**

Demographic rates

From field data, mark-recapture, and parentage analyses, we estimated growth (Fig.
²⁷⁰ 3b, SI B.3), fecundity (SI A.4), annual survival (Figs. 3c, D.5, SI B.4), lifetime
egg production ($LEP_* = 827$ [227, 2919], Fig 4a, SI B.6), and egg-recruit survival
($S_e = 0.002$ [0.0005, 0.01], Fig. D.13, SI B.7). Catalano et al. (in prep) estimated
²⁷³ the parentage (SI B.1) and dispersal kernel we used Fig. 3a, SI B.2). Details and
estimated values are in Table A1 and SI B.

Persistence metrics

²⁷⁶ Using our demographic and dispersal results, we estimated average lifetime recruit
production (LRP) across patches to be 1.74 [0.94, 5.68] (Figs. 4b, D.12). Best es-

timates of LRP_i at individual patches ranged from 0 to 3.7 (Table A5, Fig. D.8).

279 Averaged across patches, 95% of LRP estimates were ≥ 1 , which means that individuals produced enough offspring to replace themselves. However, LRP does not tell us whether those offspring settled in locations that contributed to persistence.

282 Considering retention of larvae at individual patches, we did not find any patches with $SP_i \geq 1$ (Fig. 5a), suggesting that no patch could persist in isolation. The Haina patch came closest to but was still far from self-persistence ($SP_i = 0.044$ [0.005, 0.23]).

288 For network persistence, our estimate of λ_c was 0.18 [0.09, 0.63]. None of the uncertainty distribution of λ_c was ≥ 1 (Figs. 5c, D.14), suggesting network persistence for this metapopulation was therefore extremely unlikely if not impossible.

291 Our estimate of local replacement (LR) was 0.20 [0.11, 0.65], also suggesting lack of independent persistence of our group of patches and very similar to our λ_c estimate.

294 While both LR and λ_c provide information on the ability of our patches to persist as an isolated group, they differ in their assumption of the structure of the population. LR approximates the network of patches as a single well-mixed unit, while λ_c incorporates the spatial structure of the patches and multi-generation dynamics. Results without density dependence compensation also suggested lack of persistence (SI B.8).

297 Abundance

Our estimated abundance of females over time had a positive trend for the average patch (slope = 1.08, Fig. 4a), suggesting a slight increase in population size through

time. Most individual patches also showed a positive trend in female abundance through time, though one large patch (Sitio Baybayon) showed declines (Figs. 4a, D.7s). Therefore, though the metapopulation did not exhibit network persistence, it also did not show signs of decline over the time scale of our study.

Alternative production and geographies

We then examined what conditions would be needed for this metapopulation to reach persistence. With the existing patch configuration and dispersal kernel, the system would need $\text{LRP} \geq 8.9$ (a five-fold increase) to reach network persistence. In turn, this would require a five-fold increase of egg-recruit survival (S_e) or LEP_* or an equivalent combination of increases across both. Including all arriving recruits as offspring, not just those originating within the metapopulation, LRP would be 11.1, sufficient for persistence. Similarly, our estimate of LR using all recruits arriving to the patches gave an estimate > 1 (2.21), also suggesting there was recruit-recruit replacement for the metapopulation when immigrants were included.

Another route to persistence would be with a different dispersal matrix or habitat density. If dispersal was such that the metapopulation retained all offspring produced, the study region would be persistent because $\text{LRP} > 1$. With the observed dispersal pattern, however, retaining all recruits is difficult to achieve. The coastline had a low fraction of habitat (20%) and would need to be increased to about 86% before enough offspring are retained that the point estimate of $\lambda_c > 1$ (Fig. 6a). However, widening the region while maintaining the same habitat density (20%) did not achieve persistence (Fig. 6b) unless habitat density was also increased (Fig. 6c).

As the region widens, the habitat density necessary for persistence decreases, down to 74% habitat at a region of 50 km. In contrast, allowing for larval navigation had little impact on persistence estimates (Fig. 6d), as the larger effective area of each patch was essentially offset by removing that area from the scaling that accounted for larval losses to non-habitat (P_s in eqn. 8).

327 Discussion

In this first assessment of demographic persistence of a coastal marine metapopulation, we did not find strong evidence for either self-persistence of an individual patch or network persistence of the entire 30 km area as an isolated region. This inability to persist as an isolated region does not mean that the metapopulation was declining, however. Both population trends and replacement of recruits with immigrants showed that population levels were stable or increasing slightly. Taken together, these metrics suggest that the region required input of immigrants to persist. Despite encompassing a distance substantially larger than mean dispersal, the coastline only persisted as part of a larger metapopulation.

Theory for predicting persistence within patchy habitats has suggested that we expect self-persistence when the mean dispersal distance is small relative to patch size and network persistence in groups of patches when dispersal distances are much larger than patch sizes and where the proportion of habitat in the landscape is about 10-40% (depending on the particular species, population, and maximum reproductive rate, Botsford et al., 2019). Individual patches in the focal metapopulation were too small for self-persistence, but the 30 km region we sampled was about triple the

mean dispersal distance of yellowtail anemonefish estimated from previous genetic work (around 9 km, Pinsky et al., 2010) and from our parentage analyses (8.2 km, Catalano et al., in prep). Rather than a continuous patch, however, the region was only about 20% habitat. Low habitat may result at least in part from habitat declines over recent decades, based on interviews with fishers in the early 2000s (Jennifer Selgraeth, pers. comm.). Increasing the proportion of coastline with habitat in sensitivity tests, however, suggested that even 40% habitat coverage would not be sufficient to achieve persistence and this metapopulation would require almost continuous habitat to persist. Similar to fish on small patches in the Caribbean (Johnson et al., 2018), this anemonefish metapopulation depends on the production and connectivity of outside patches. One possible path to persistence would be through nearby patches with higher egg production or survival. In such a case, even a small increase in area could create a persistent network. Deeper reefs, for example, are often healthier than shallower reefs (Cinner et al., 2016); LRP_i is highest at our deepest patch, Tomakin Dako. In this system, offshore reefs at Cuatro Islas or the Camotes Islands, for example, with higher coral cover and less silt, could have higher anemonefish survival and contribute disproportionately to regional metapopulation persistence.

Our finding of a lack of isolated persistence differs markedly from persistence findings of other reef fish metapopulations. On reefs surrounding Kimbe Island, Salles et al. (2015) report self-persistence of individual anemonefish subpopulations in lagoons that were of similar size (approximately 100-500m long) to our individual patches, as well as network persistence of the only-800m wide metapopulation around

the island. This persistence finding is at a dramatically smaller scale than for our focal population in the Philippines. Additionally, Johnson et al. (2018) estimated
369 that four reefs of a combined area of only 2.6 km² (4 65 ha patches) would be sufficient for network persistence of a damselfish metapopulation across multiple islands in the Bahamas. This area is equivalent to a coastline section shorter than
372 our sampling region (approximately 30 km long and 0.1 km wide). To persist, these two offshore metapopulations either had much higher retention of recruits or higher LRP than did our coastline patches. Though lack of sufficient connectivity and
375 retention is thought to inhibit network persistence in some systems (e.g., insufficient retention of offspring within reserves for eastern oysters (*Crassostrea virginica*) in North Carolina; Puckett and Eggleston, 2016), production of surviving recruits seems
378 the likelier explanation in this case. Recruit production was lower in the Philippines than in the Kimbe Island populations, where Salles et al. (2020) estimated that an average individual produced 0.54 offspring over two years that recruited back to the
381 natal population, more than twice our similar estimate of local replacement (LR = 0.20), which considered lifetime rather than biennial production of locally-recruiting offspring. Lower production at our patches could be due to lower egg production,
384 slower growth, or lower adult survival, all likely affected by habitat quality (e.g. Salles et al., 2020; Hayashi et al., 2019). Our study system was near a populated coastline and experienced anthropogenic effects, including pollution and silt, that
387 can reduce demographic rates. Adult survival, for example, was lower at the two patches just downstream of a gravel mine (N. and S. Magbangon in Fig. B.3). Even at our higher-survival patches (38% annual survival for a 6cm fish and 53% for a

390 10cm fish at Tomakin Dako, for example), survival was lower than estimates from
the populations at Kimbe Island (85% annual survival, Salles et al., 2015). Estimates
of annual survival in other reef fish species are closer to the lower survival we found
393 for yellowtail anemonefish than the higher survival of *A. percula* at Kimbe Island
(approximately 30% annual survival for bluehead wrasse (*Thalassoma bifasciatum*)
and bicolour damselfish (*Stegastes partitus*), respectively; Warner and Hughes, 1988;
396 Figueira et al., 2008). Metapopulation studies in other reef fish (e.g., Figueira, 2009)
and marine species more broadly (Carson et al., 2011) are highly sensitive to adult
survival and other demographic parameters.

399 Temporal variability in demographic or dispersal parameters on a time scale
longer than our sampling could also enable persistence of our patches in isolation
(similar to the storage effect, Warner and Chesson, 1985) rather than as part of a
402 larger metapopulation. Successful recruitment events on the decadal scale, for exam-
ple, sustain rockfish populations on the west coast of the United States through the
intervening weak recruitment years (e.g. Tolimieri and Levin, 2005). Our study could
405 have missed a particularly strong recruitment event driven by variable ocean con-
nectivity (simulations suggest that 20 years are necessary to capture the full extent
of ocean variability in the Coral Triangle region surrounding our patches; Thompson
408 et al., 2018). Strong recruitment would need to occur at least once a generation
to maintain patch populations without switching to colonization and extinction dy-
namics, however, which we do not see. Our study likely spans the generation time
411 of a yellowtail anemonefish (roughly 5 years) so variable strong recruitment, while
possible, is unlikely to sustain our populations.

Understanding our region in the context of broader metapopulation theory requires reconciling replacement-based persistence analysis with classic colonization-extinction and source-sink dynamics. At the patch level, many marine metapopulations do not exhibit the colonization-extinction dynamics (or do only on a decades to centuries timescale, Smedbol et al., 2002) that underpin our understanding of many terrestrial metapopulations (e.g, Hanski, 1998; Moilanen et al., 1998) and instead consist of continuously-occupied patches connected by dispersal (Kritzer and Sale, 2006). Because dispersal is so widespread, patches in marine systems are not easily classified as sources or sinks in the classical fashion (Figueira and Crowder, 2006; White and Samhouri, 2011). For example, despite being unable to persist in isolation, our region is not technically a sink (Pulliam, 1988) because $LRP > 1$. For metapopulations, lack of self-persistence can have two causes: reproduction does not balance mortality losses within a patch (a sink) or sufficient recruits are produced but not retained (as we found in the Philippines). Metapopulations likely lie on a continuum between extinction-colonization dynamics and exchange among populated patches (Kritzer and Sale, 2006) but the latter may be a more practical approach to characterizing dynamics for metapopulations in which exchange is frequent relative to organisms' generations times (Hastings and Botsford, 2006).

Density dependence also presents a sampling challenge. Persistence criteria (Hastings and Botsford, 2006; Burgess et al., 2014) ask whether a population at low abundance can grow and recover rather than going extinct. Density dependence is often ignored at low abundances (Botsford et al., 2019) so is not explicitly considered in persistence metrics. In real populations, however, it can be challenging to estimate

density-independent demographic rates because density dependence is occurring in the population as it is sampled during dispersal (Nowicki and Vrabec, 2011) and reproduction (Rodenhouse et al., 2003). In yellowtail anemonefish, density dependence is likely most important immediately post-settlement, as it is for many species, including corals, trees, and butterflies (Vermeij and Sandin, 2008; Harms et al., 2000; Nowicki et al., 2009). However, density dependence could continue to be important throughout the life history due to social hierarchies in anemonefish colonies (Buston and Elith, 2011). To avoid competition within the colony, fish in the pre-reproductive queue may have lower growth and survival than fish alone on an anemone (Buston, 2003b,a), suggesting higher growth and survival, and therefore LRP, in the absence of density dependence. Our calculations of self-persistence in this paper did not account for post-settlement density dependence, which would be an interesting area of further research.

Understanding persistence is critical for the management of spatial populations, such as siting marine protected areas (Kaplan et al., 2009), assessing habitat fragmentation risks (Smith and Hellmann, 2002; Fahrig, 2001) and conserving species in the face of climate change (Coleman et al., 2017; Fuller et al., 2015). Though models and theory provide us with expectations, we are only recently beginning to be able to tackle these questions of persistence empirically in model systems such as anemonefish and other sedentary tropical reef fish (Salles et al., 2015; Johnson et al., 2018). With parentage analyses now being extended to temperate marine species (Baetscher et al., 2019) and a better understanding of how biophysical models compare to larval dispersal patterns (Bode et al., 2019), we are beginning to move

⁴⁵⁹ beyond model species and investigate persistence in harvested and spatially-managed systems (Garavelli et al., 2018). Our study shows the importance of long-term sampling and careful consideration of the demographic and sampling processes that affect persistence calculations in order to determine persistence mechanisms and assess persistence state to understand marine population dynamics in empirical systems.

Figures

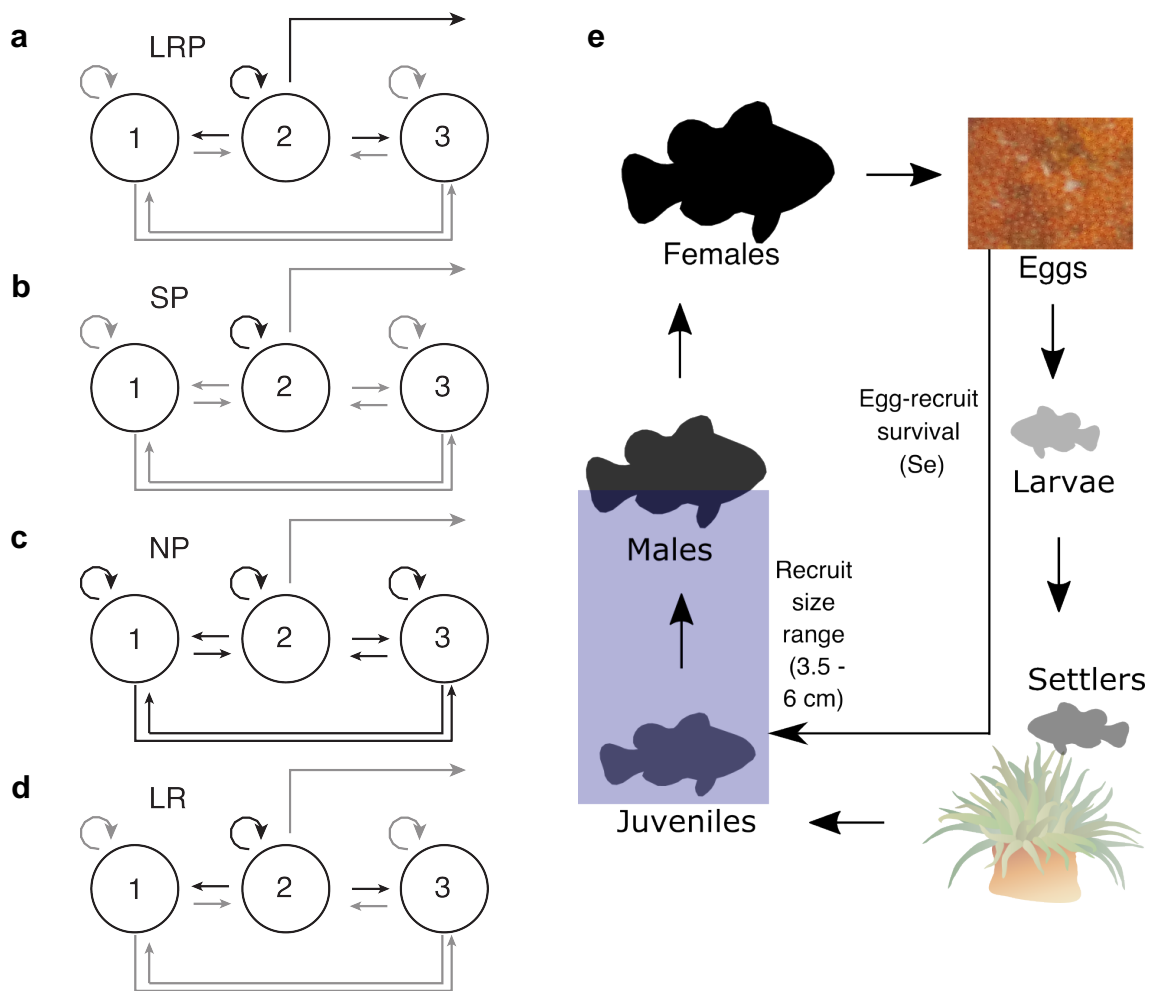


Figure 1: Schematics of the persistence metrics (a-d): a) lifetime recruit production (LRP, eqn. 1), b) self-persistence (SP, eqn. 2), c) network persistence (λ_c , first eigenvalue of eqn. 3), and d) local replacement (LR, eqn. 4). e) The life cycle of yellowtail anemonefish, including the range of sizes considered to be recruits (recruit definition in SI A.1).

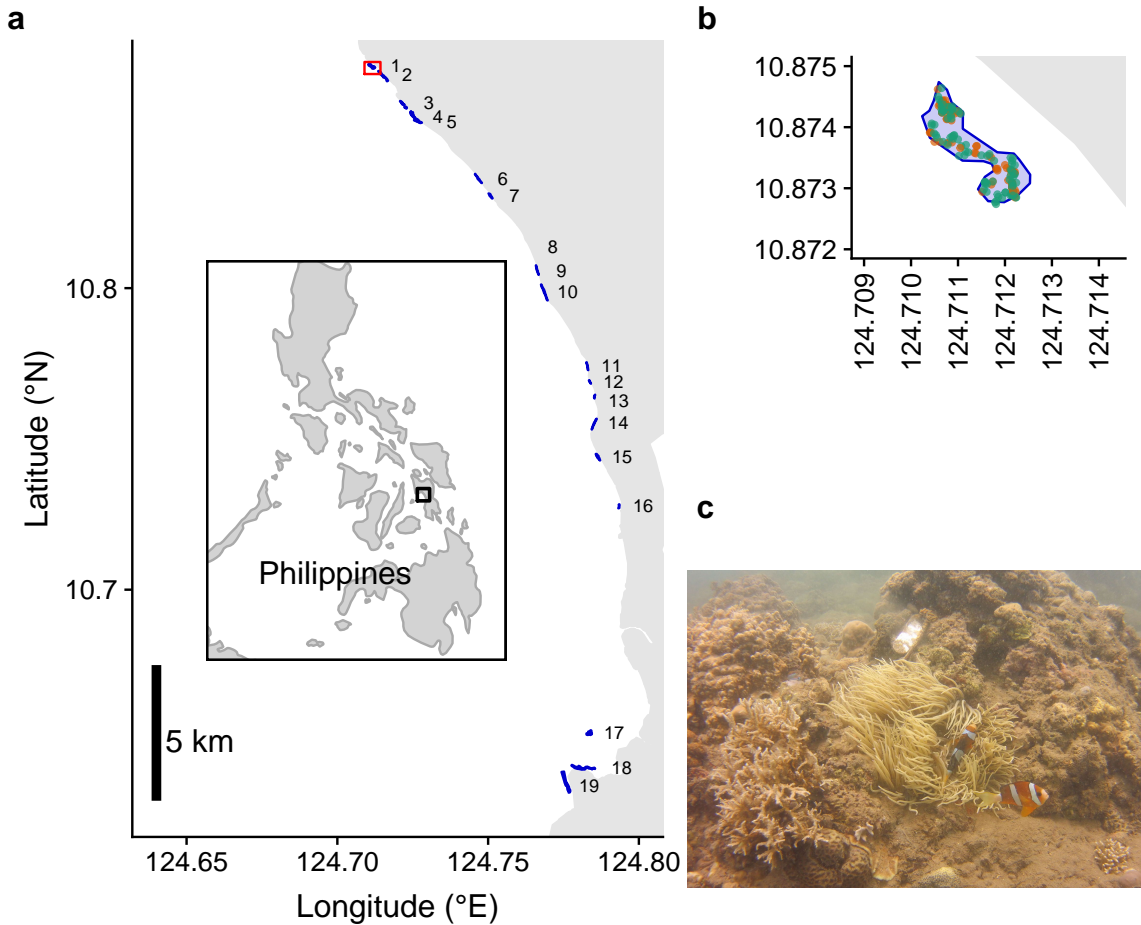


Figure 2: a) Map of the patches along the coast of Leyte in the Philippines. From north to south, the patches are: 1) Palanas, 2) Wangag, 3) North Magbangon, 4) South Magbangon, 5) Cabatoan, 6) Caridad Cemetery, 7) Caridad Proper, 8) Hicgop South, 9) Sitio Tugas, 10) Elementary School, 11) Sitio Lonas, 12) San Agustín, 13) Poroc San Flower, 14) Poroc Rose, 15) Visca, 16) Gabas, 17) Tomakin Dako, 18) Haina, and 19) Sitio Baybayon. b) Zoomed-in map of the northern-most patch, Palanas (red box on map), to show anemone arrangement. Anemones are colored as occupied by yellowtail anemonefish (green) or unoccupied by anemonefish (orange). c) An example anemone occupied by yellowtail anemonefish in a typical habitat. The metal anemone tag is visible just above the anemone on the rock.

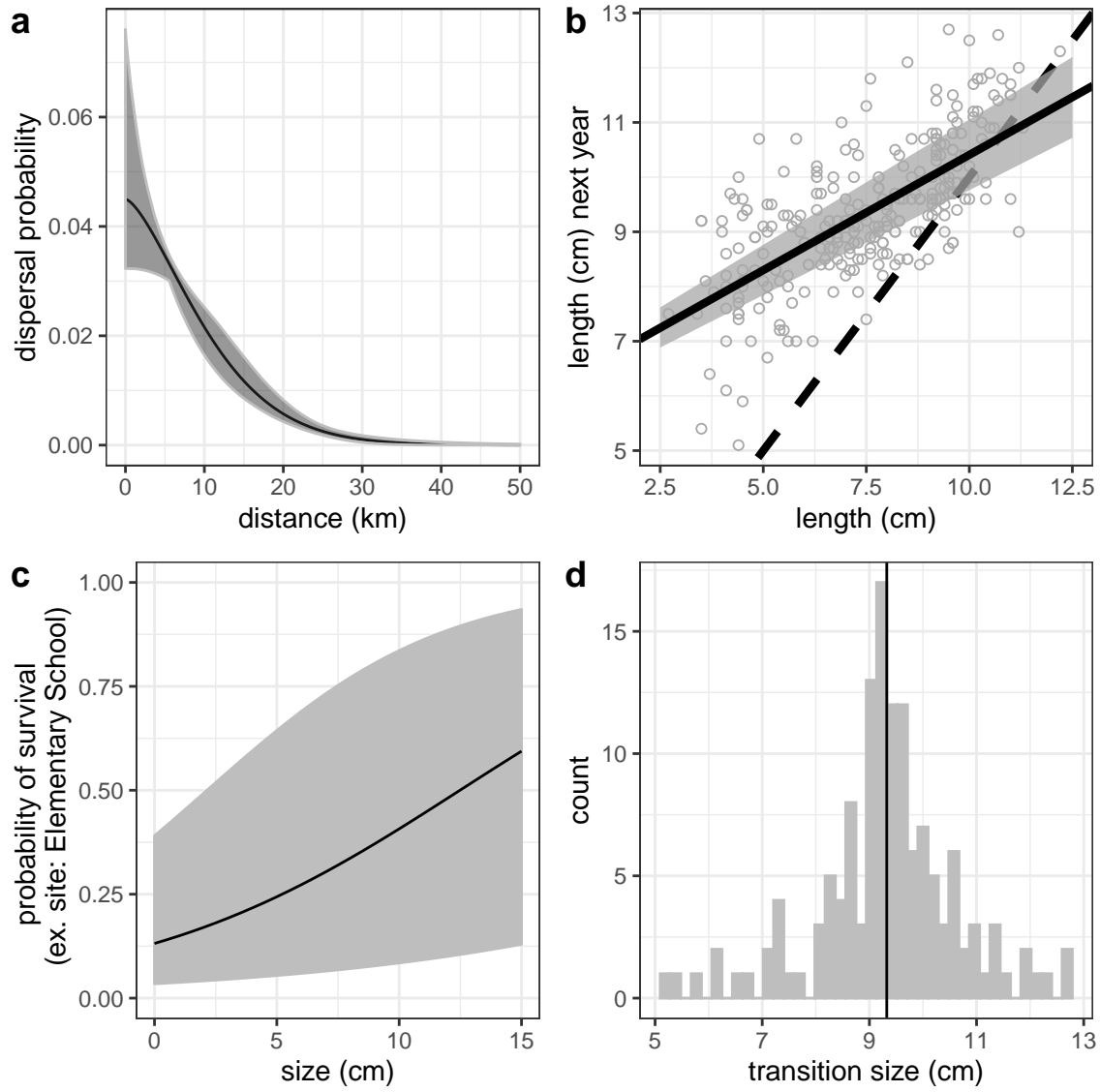


Figure 3: Estimates (solid black line) and uncertainty (grey) for a) dispersal (eqn. 5), b) growth (eqn. 6), including a dashed 1:1 line, c) post-recruit annual survival (eqn. B.1) at Elementary School as an example patch, and d) raw data of fish size at female transition (L_f in eqn. A.1).

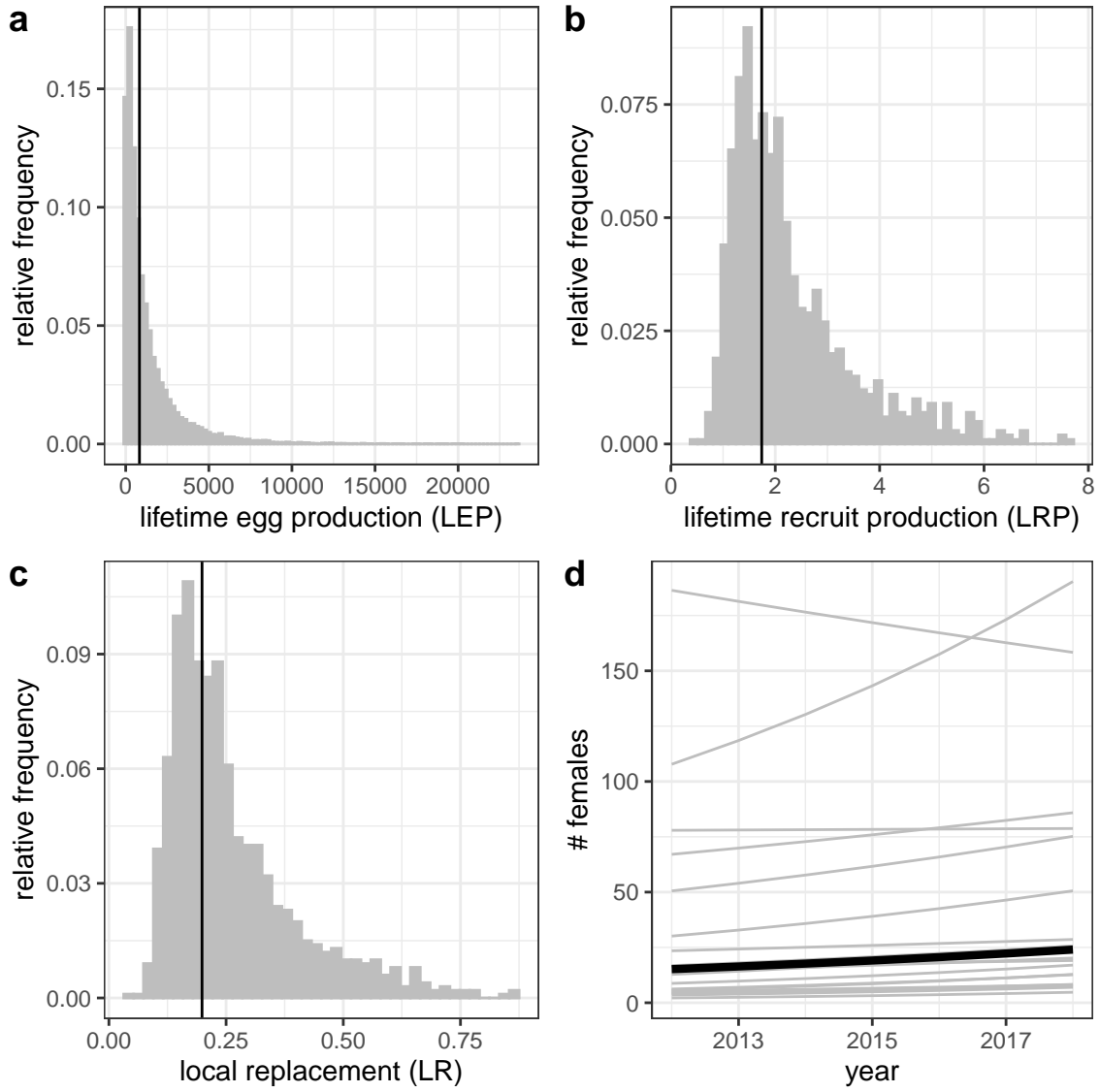


Figure 4: Estimates of a) individual-patch LEP_i (eqn. 7) for all patches with the point estimate averaged across patches (LEP_* , black line), b) average LRP across patches (eqn. 1), c) local replacement (eqn. 4), showing the point estimate (black solid line) and range of estimates considering uncertainty in the inputs (grey). Estimates of LRP and LR include compensation for density-dependent mortality in early life stages. d) Estimated abundance of females over time at each individual patch (grey lines) and for an average patch (black line).

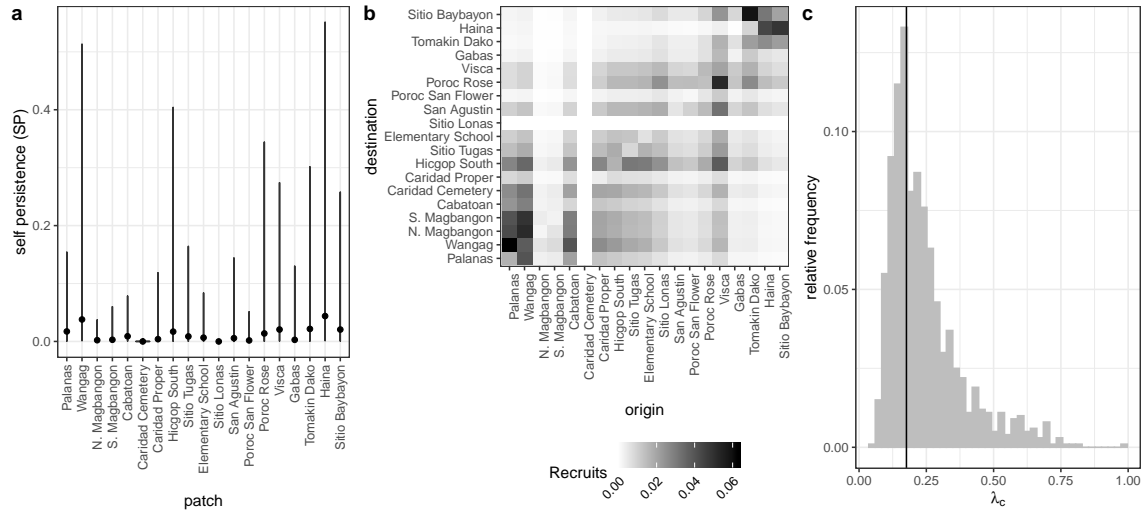


Figure 5: Values of a) self-persistence (SP, eqn. 2), b) realized connectivity among patches ($C_{i,j}$, eqn. 3), and c) network persistence (λ_c , first eigenvalue of eqn. 3). All estimates include compensation for density dependence in early life stages. For self-persistence (a) and network persistence (c), the best estimate is shown in black (point for (a), line for (c)) and the range of estimates considering uncertainty is shown in grey.

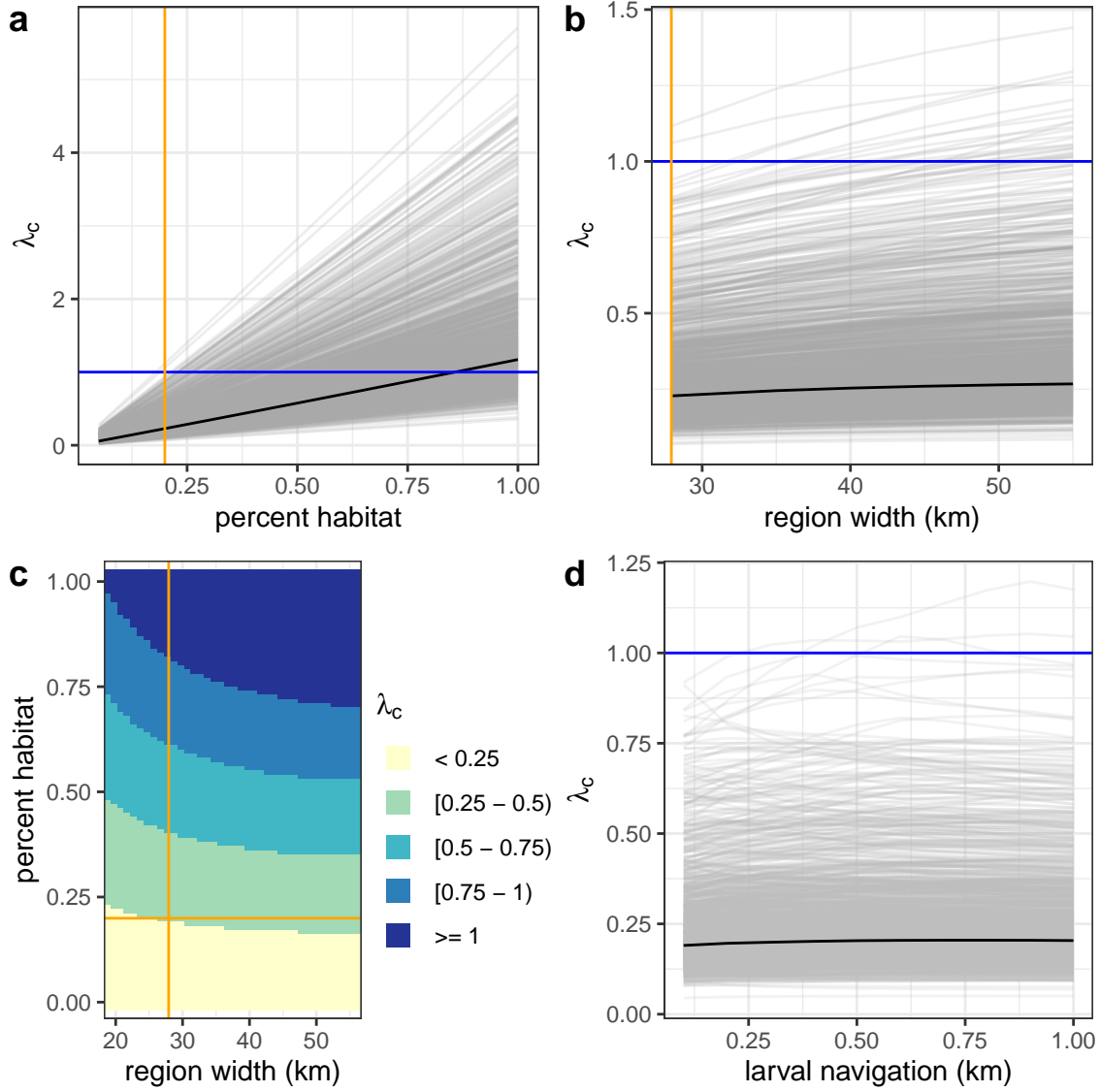


Figure 6: Sensitivity of network persistence (λ_c) to a) the proportion of the sampling region that is habitat (P_s), b) the width of a region with the same proportion habitat (20%), c) the region width and proportion habitat simultaneously, and d) larval navigation, where up to a 1 km buffer is added to the patch edges. The estimate is in black and each estimate with uncertainty is a grey line. The orange lines show the actual proportion habitat (20%) and region width (27 km) and the blue line shows the persistence threshold where $\lambda_c = 1$.

465

Appendix

A Supplemental Methods

A.1 Defining recruit and census stage

468 When assessing persistence, we must consider mortality and reproduction that occurs
across the entire life cycle to determine whether an individual is replacing itself with
an individual that reaches the same life stage (Burgess et al., 2014). We defined a
471 recruit to be a juvenile individual that has settled on the reef within the previous
year, which also encompasses the size of fish we were first able to sample (3.5-6.0 cm
for parentage studies) (Figs. 1e, D.1). In theory, it does not matter how we defined
474 recruit as long as we used that definition in our calculations of both egg-recruit
survival (eqn. 8) and LEP (eqn. 7). In our system, however, while it is straightforward
to calculate LEP from any size, we did not have enough tagged recruits to reliably
477 estimate survival from an egg to different recruit sizes. Instead, we chose the mean
size of offspring matched in the parentage study as our best estimate of the size
of a recruit ($\text{size}_{\text{recruit}} = 4.4 \text{ cm}$) and tested sensitivity to different recruit sizes by
480 sampling from a uniform distribution over the sizes the recruit stage covers (3.5-6
cm, Table A1, Figs. D.11-D.14).

A.2 Self persistence (SP)

483 Our equation for SP (eqn. 2) is a modification of that used in Burgess et al. (2014),
which uses LEP to represent offspring produced and local retention (the number

of surviving recruits that disperse back to the natal patch divided by the number
486 of eggs produced by the natal patch) to capture egg-recruit survival and dispersal
combined: LEP x local retention ≥ 1 . We modify this to include egg-recruit survival
in the offspring term instead, using LRP in place of LEP and probability of dispersal
489 ($p_{i,i}$) in place of local retention.

A.3 Growth and survival

To include size in the mark-recapture models for survival and recapture probability,
492 we estimated sizes for fish in years when they were not recaptured. We used the
growth model (eqn. 6) and the size recorded or estimated in the previous year to
estimate the size of fish not recaptured in a particular year. Fish were not well-mixed
495 at our patches, and divers needed to swim near an anemone to have a reasonable
chance of capturing the fish on it. Therefore we also included a distance effect on
recapture probability (eqn. B.2, Table A3). We used diver GPS tracks to estimate
498 the minimum distance between a diver and the anemone where the fish was first
caught for each tagged fish in each sample year.

We compared the fit of the models using a modified version of the Akaike information criterion that reduces the potential for overfitting with small sample sizes
501 (AICc) and selected the model with the lowest AICc value (Table A3).

A.4 Fecundity

504 We used a size-dependent fecundity relationship determined using photos of egg
clutches and females from field sampling, where the number of eggs per clutch (E_c) is

exponentially related to the length in cm of the female (L) with size effect $\beta_l = 2.388$,
 507 intercept $b = 1.174$, and egg age effect $\beta_e = -0.608$ dependent on if the eggs were old
 enough to have visible eyes. For fish larger or equal to the transition to female size
 510 L_f , we multiplied the number of eyed eggs per clutch by the number of clutches per
 f for a female of length L :

$$f(L) = \begin{cases} 0, & \text{if } L < L_f \\ c_e * e^{\beta_l \ln(L) + \beta_e [\text{eyed}] + b}, & L \geq L_f. \end{cases} \quad (\text{A.1})$$

A.5 Lifetime egg production (LEP)

513 To compute LEP, we discretized time and size (in eqn. 7) and summed across the
 matrix. When entering the starting individual into the matrix, we used 0.1 as the
 standard deviation of size to spread out the starting individual across size bins. To
 516 account for differences in growth rates across fish, we used the size determined by
 the growth curve (eqn. 6) as the mean along with an estimate of spread (size_{sd})
 when projecting the size distribution of the fish in the next year. To estimate size_{sd} ,
 519 we selected fish within 0.1 cm of the mean size at the first capture point for fish
 recaptured a year later (7.4-7.6 cm). We used the standard deviation of the sizes of
 those fish when they were recaptured one year later as size_{sd} (=1.45) (Table A1).

522 LEP was estimated by patch (LEP_i) because each patch has a different estimate
 of adult survival. We also present the average LEP across patches, noted as LEP_*
 (Fig. 4b) and used to estimate average LRP and LR for the metapopulation (Fig.

525 4c, d).

To estimate egg-recruit survival (S_e), we used the expected lifetime egg production for a fish that has already survived to reach parent size (6.0 cm) so L_s in eqn. 7
528 = 6.0, rather than 3.5. We used the average LEP for parent-sized fish across patches,
noted as LEPp.

A.6 Accounting for density dependence

531 In 2015 and 2017, we did a more thorough survey of anemones at sampled patches
and noted anemones occupied by yellowtail anemonefish, occupied by other species of
anemonefish, and unoccupied by anemonefish. We found the proportion of anemones
534 occupied by yellowtail anemonefish (p_A) and the proportion of anemones unoccupied
by any anemonefish (p_U) for all patches combined and averaged across the two sample
years. We used these average proportions to estimate the proportional increase (DD)
537 in unoccupied anemones if all anemones occupied by yellowtail anemonefish were
unoccupied as described in the main text. We did not consider uncertainty in the
effect of density dependence.

540 A.7 Alternative geographies and larval navigation

A.7.0.1 Larval navigation

In our sensitivity test for larval navigation and swimming abilities, we added a buffer
543 ranging from 0 - 1 km to the edges of the destination patches when determining
probability of dispersal between patches. To avoid overlapping shadows of effective
area of neighboring patches, we added no more than half the distance between two

adjacent patches to each patch. The buffers also changed the proportion of the sampling region that was habitat (P_h , see SI A.8.0.4), as we considered the buffer areas to be habitat as well, and affected the scaling of recruits (SI A.8) in egg-recruit survival (eqn. 8).

A.8 Scaling up recruits

To estimate the total number of offspring produced by genotyped parents that survived to recruitment, we scaled up the number of matched offspring caught during sampling (R_m) to account for recruits our sampling could have missed (Fig. D.2). We scaled up by 1) the cumulative proportion of habitat we sampled at our patches over time (P_h) to account for recruits at anemones we did not sample (details in SI A.8.0.1), 2) the probability of capturing a fish if we sampled its anemone (P_c) to account for fish that escaped during sampling (details in SI A.8.0.2), 3) the proportion of the dispersal kernel from our patches covered within our sampling region (P_d) to account for fish that dispersed outside of our sampling area (Fig. D.4, details in SI A.8.0.3), and 4) the proportion of our sampling region that was habitat (P_s) to avoid counting mortality of fish dispersing to non-habitat within our region twice (details in SI A.8.0.4). The latter term is important because mortality from dispersing to non-habitat is both in the estimate of total recruits (numerator of eqn. 8) and in the integrated dispersal kernel (eqn. 5).

A.8.0.1 Proportion of habitat sampled (P_h)

We used tagged anemones to estimate the proportion of habitat we sampled within our patches. We tagged each anemone that was home to yellowtail anemonefish with a metal tag, which is relatively permanent and easy to re-sight (the anemone tag is visible above the anemone in Fig. 2c). We therefore considered the total number of metal-tagged anemones at a patch to be the habitat present. We used proportion of anemones rather than proportion of total patch area because anemones, and therefore habitat quality, were unevenly distributed across each patch; areas we did not visit typically had a lower anemone density than the areas we did sample.

To scale the number of sampled offspring from genotyped parents (R_m) to account for areas of our patches we did not sample, we used the overall proportion habitat sampled across all patches and sampling years (P_h). We summed the number of metal-tagged anemones we visited across all patches and years, then divided by the number of anemones we could have sampled (the sum of total metal-tagged anemones across all patches multiplied by the number of sampling years). We did not consider uncertainty in the proportion of habitat sampled.

A.8.0.2 Probability of capturing a fish, from recapture dives (P_c)

We used the probability of capturing a fish to scale up the number of sampled offspring from genotyped parents (R_m) to account for recruits we missed by failing to capture them. To estimate the probability of capturing a fish given that we sampled its anemone (P_c), we used mark-recapture data from recapture dives done

within a sampling season. During some of the sampling years, we intentionally re-sampled some locations within a few weeks of the original sampling dives. We
588 assumed that the probability of recapturing a fish on a recapture dive was the same as capturing a fish on a sampling dive, essentially that there was no mortality in the weeks between dives and that the fish did not alter their behavior towards divers.
591 For each recapture dive, we used GPS tracks of the divers to identify the anemones covered in the recapture dive and the set of PIT-tagged fish encountered on those anemones during the original sampling dives. We estimated the probability of capture
594 P_c as the number of tagged fish re-caught during the capture dive m_2 divided by the total number of fish caught on the recapture dive n_2 : $P_c = \frac{m_2}{n_2}$.

We used the mean P_c across all 14 recapture dives, covering 10 patches over three
597 sampling seasons (2016, 2017, 2018), as our best estimate. Uncertainty details are in SI A.9.0.6.

A.8.0.3 Proportion of dispersal kernel area sampled (P_d)

600 To account for recruits that dispersed outside our sampling region, we found the proportion of the dispersal kernels from all parents that fell within our sampling region (Fig. D.4). For each patch i , we found the area under the kernel (A_i) from
603 the center of the patch to the north edge of the sampling area ($d_{N,i}$) (northern-most tagged anemone at Palanas, the northern-most patch) and from the center of the patch to the south edge of the sampling area ($d_{S,i}$) (southern-most tagged anemone
606 at Sitio Baybayon, the southern-most patch), then multiplied by the number of genotyped parents at that patch (N_{g_i}):

$$A_i = N_{g_i} \frac{z\theta}{2\gamma(\frac{1}{\theta})} \left(\int_0^{d_N} z e^{-(zd)^\theta} dd + \int_0^{d_S} z e^{-(zd)^\theta} dd \right). \quad (\text{A.2})$$

We added the areas together, then divided by the total number of genotyped parents (N_g) to get the proportion of the total dispersal kernel area covered by our sampling region (P_d):

$$P_d = \frac{\sum_{i=1}^{19} A_i}{N_g}. \quad (\text{A.3})$$

We did not consider uncertainty in P_d .

612 A.8.0.4 Proportion habitat in sampling area (P_s)

To avoid implicitly counting mortality due to larvae settling on non-habitat twice - once in scaling up our matched recruits (who settled on habitat) and once in integrating the dispersal kernel - we scaled the estimate of total recruits produced by parents on our patches by the proportion of our sampling region that was habitat (P_s). We found P_s by summing the lengths of all the patches, which run approximately north-south, and dividing by the total north-south distance of our sampling region, giving $P_s = 0.20$. We assumed that larvae were unable to navigate to habitat if they dispersed to an unsuitable area but relaxed that assumption in our sensitivity tests (SI 621 A.7.0.1) because anemonefish larvae do likely have some ability both to sense good settlement areas by detecting host anemones (Elliott et al., 1995; Arvedlund et al., 1999) or conspecifics (e.g., Lecchini et al., 2005, for coral reef fish more broadly), and 624 to swim in a particular direction (e.g., Bellwood and Fisher, 2001; Fisher, 2005).

A.9 Characterizing uncertainty

A.9.0.1 Dispersal kernel

- 627 To account for uncertainty in the dispersal kernel, we used sets of the shape parameter
 θ and the scale parameter K_d that represented the span of the 95% confidence interval
when K_d and θ were estimated jointly (Table A1, Fig. 3a, Catalano et al., in prep).
630 We randomly sampled pairs of θ and K_d parameters from the distribution, weighted
by the log-likelihood.

A.9.0.2 Growth

- 633 We used the first and second capture lengths for fish that were recaptured after a year
(within 345 to 385 days) to estimate L_∞ and k (using eqn. 6). For fish recaptured
more than once, we randomly selected only one recapture period from each to use
636 to estimate the von Bertalanffy parameters and repeated the random selection and
estimate 1000 times. We found the mean estimates ($L_\infty = 10.70$ cm, $k = 0.864$) and
mean standard error of those fits, then sampled from within that range to generate a
639 set of von Bertalanffy growth curves to use in our LEP calculations (Figs. 3b, D.3b,
Table A1).

A.9.0.3 Survival

- 642 We incorporated uncertainty in adult survival by sampling from within the 95%
confidence limits for the patch-based survival estimates and size effect on survival
as estimated by the lowest AICc model from MARK (Table A2, Fig. D.5). For the

645 simulations for the alternative geographies and larval navigation, we used the survival estimate and 95% range for the patch with median survival (Elementary School).

A.9.0.4 Size of transition to female (L_f)

648 To incorporate uncertainty in the size at which male fish transition to female (L_f), we sampled with replacement directly from the sizes at which recaptured fish were first captured as female (5.2 cm - 12.7 cm) (Fig. 3d). Reproductive output is only counted
651 once fish reach the female stage, so L_f affects fecundity (eqn. A.1) and therefore the fecundity kernel in calculating lifetime egg production (f_L in eqn. 7).

A.9.0.5 Recruit size (size_{recruit})

654 We incorporated uncertainty in the size of a recruit (size_{recruit}) by sampling from a uniform distribution across the ranges of possible sizes of recruits for the parentage analysis (3.5-6.0 cm) (Fig. D.3a). Recruit size enters into LEP as the starting size
657 of the individual fish.

A.9.0.6 Probability of capturing a fish (P_c)

To consider uncertainty in the probability of capturing a fish given that we sampled its anemone (P_c), we represented the probability of capture as a beta distribution, using the mean μ_{P_c} and variance V_{P_c} of the set of 14 values calculated from individual recapture dives to find the appropriate α_{P_c} and β_{P_c} parameters, where
660

$$\alpha_{P_c} = \left(\frac{1 - \mu_{P_c}}{V_{P_c}} - \frac{1}{\mu_{P_c}} \right) \mu_{P_c}^2 \quad (\text{A.4})$$

$$\beta_{P_c} = \alpha_{\mu_{P_c}} \times \frac{1}{\mu_{P_c} - 1}. \quad (\text{A.5})$$

663 The mean of the individual capture probability values was $\mu_{P_c} = 0.56$, with
variance $V_{P_c} = 0.069$, giving beta distribution parameters $\alpha_{P_c} = 1.44$ and $\beta_{P_c} = 1.13$.
We sampled 1000 values from the beta distribution, then truncated the sample to
666 include only values larger or equal to the lowest value of P_c estimated from an
individual dive (0.20), to avoid unrealistically low values randomly sampled from the
distribution. We then sampled with replacement from the truncated set to get a
669 vector of 1000 values (Fig. D.3c). P_c is one of the scaling factors in the estimate of
egg-recruit survival (eqn. 8), accounting for recruits we missed by failing to capture
them.

672 A.9.0.7 Lifetime Egg Production (LEP)

Uncertainty in lifetime egg production enters through adult survival (SI A.9.0.3),
growth (SI A.9.0.2), and the size of a recruit (SI A.9.0.5), all of which affect the size
675 distribution v_L in eqn. 7. Additionally, uncertainty in the size of transition to female
(L_f , SI A.9.0.4) affects the fecundity kernel f_L in eqn. 7. We show the contribution
of uncertainty of each input in Fig. D.11.

678 **A.9.0.8 Egg-recruit survival (S_e)**

In estimating egg-recruit survival (S_e), we considered uncertainty in the number of offspring assigned to parents (R_m) and in the probability of capturing a fish (P_c).
681 For offspring assigned to parents, we generated a set of values for the number of assigned offspring using a random binomial, with the number of genotyped offspring (791) as the number of trials and the assignment rate from the parentage analysis
684 (0.090) as the probability of success on each trial (Catalano et al., in prep), (Fig. D.3d). Uncertainty in probability of capture P_c is described in SI A.9.0.6. We show the contribution of uncertainty of each input in Fig. D.13.

687 **B Supplemental Results**

B.1 Parentage

From the genetic work and parentage analysis done in Catalano et al. (in prep), we
690 genotyped 1729 potential parents, genotyped 791 potential offspring (recruits), and
matched 71 offspring to parents, with an assignment rate of 9%. In estimates with
uncertainty, the middle 95% distribution of matched offspring was 55 to 87 (Fig.
693 D.3d, Table A1).

B.2 Dispersal kernel

We used the dispersal kernel estimated for all years together in Catalano et al. (in
696 prep) (eqn. 5), with $K_d = -2.51$ and $\theta = 1.49$. Using the 95% confidence surface
when K_d and θ were estimated jointly to incorporate uncertainty (SI A.9.0.1), K_d
ranged from -2.86 to -1.82 and θ from 0.87 to 2.46 (Fig. 3a, Table A1).

699 **B.3 Growth**

From the mark-recapture analysis of tagged and genotyped fish, we estimated mean
values of $L_\infty = 10.70$ cm with uncertainty bounds 9.81-11.65 and $k = 0.864$ with
702 uncertainty bounds 0.80-0.91 for the von Bertalanffy growth curve parameters (eqn.
6, Fig. 3b, Table A1).

B.4 Survival

705 The best model for post-recruitment annual survival ϕ on a log-odds scale had a positive size effect ($b_a = 0.15 \pm 0.029$ SE) with intercepts b_{ϕ_i} varying by patch (eqn. B.1, Fig. D.5, Table A2):

$$\log\left(\frac{\phi}{1 - \phi}\right) = b_{\phi_i} + b_a \text{size.} \quad (\text{B.1})$$

708 The accompanying best model for recapture probability p_r on a log-odds scale had a negative effect of size ($b_1 = -0.16 \pm 0.09$ SE) and a negative effect of diver distance from anemone ($b_2 = -0.15 \pm 0.02$ SE), with intercept $b_{p_r} = 2.14 \pm 0.87$ SE
711 (eqn. B.2, Fig. D.6):

$$\log\left(\frac{p_r}{1 - p_r}\right) = b_{p_r} + b_1 \text{size} + b_2 d. \quad (\text{B.2})$$

This suggests divers were less likely to recapture larger fish, which are stronger swimmers and more likely to flee when divers approach, and those at anemones far
714 from areas sampled.

B.5 Scaling factors

The proportion of habitat at patches sampled over time (P_h) was 0.41, the proportion
717 of the region that was habitat (P_s) was 0.20, the proportion of the dispersal kernel that was within the sampling region (P_d) was 0.57, and the probability of capturing a fish given that its anemone was sampled (P_c) was 0.56 [0.22, 0.97] (Fig. D.3c, Table

720 A1).

B.6 Lifetime egg production (LEP)

We calculated an average value of LEP (LEP_*) across patches of 827 [227, 2919] eggs
723 (Fig. 4b), with best estimate values at individual patches that ranged from 0 to 1760
eggs (Table A5). Uncertainty in adult survival had the largest effect on LEP (Fig.
D.11), which corresponds to longer-surviving individuals having more opportunities
726 to reproduce at larger sizes.

B.7 Egg-recruit survival (S_e)

We estimated egg-recruit survival S_e to be $0.002 [5 \times 10^{-4}, 0.01]$ when we accounted
729 for density dependence in our data. Uncertainty in the size of transition to breeding
female L_f had the largest effect on egg-recruit survival (Fig. D.13); the larger the
transition size to female, the fewer tagged eggs we estimated were produced by our
732 genotyped parents and the higher the estimate of egg-recruit survival. This differs
from our finding above that adult survival had the largest effect on LEP because the
starting size of the individual considered is lower when we estimate LEP for a recruit
735 (4.4 cm, 3.5-6.0cm range) than for a parent (6.0cm). Fish considered parents in our
parentage analysis have already survived one or more years since recruiting so the
transition to breeding female plays a larger role in the number of eggs they are likely
738 to produce than for fish who have just recruited.

B.8 Persistence metrics without compensation for density dependence

⁷⁴¹ Estimating persistence metrics without compensating for density dependence in our data (subscript DD) gave us an understanding of whether individuals at our patches were able to replace themselves and whether our patches would persist in isolation at ⁷⁴⁴ the current abundance levels, rather than at low abundance. Without compensation for early life density dependence, all of our metrics showed that the set of patches we sampled was less likely to persist as an isolated network than the metrics for low ⁷⁴⁷ abundance. We estimated egg-recruit survival ($S_{e_{DD}}$) to be 0.001 [3×10^{-4} , 0.005] and average lifetime recruit production across patches (LRP_{DD}) to be 0.96 [0.52, 3.14], with 57% of LRP_{DD} estimates ≥ 1 (Fig. D.9a). Our estimate of local replacement ⁷⁵⁰ (LR_{DD}), which estimates replacement for recruits from our patches returning to our patches implicitly including dispersal, was 0.11 [0.06, 0.36] (Fig. D.9b).

⁷⁵³ When we calculated LR using all arriving recruits to our patches, however, rather than just those originating there, the best estimate was > 1 (1.22), suggesting that there was recruit-recruit replacement at our patches when we included immigrant recruits, even at current population levels when density dependence was present.

⁷⁵⁶ We did not find any patches with a best estimate of $SP_{DD} \geq 1$ or with uncertainty bounds that reached or exceeded 1 (Figs. D.10a). Our best estimate of the dominant eigenvalue of the realized connectivity matrix $\lambda_{c_{DD}}$ was 0.10 [0.05, 0.35] with 0% of ⁷⁵⁹ estimates where $\lambda_{c_{DD}} \geq 1$ (Fig. D.10c).

C Supplemental Tables

Table A1: Summary of parameter symbols, definitions, and values, including sections and equations where each are described in detail.

Parameter	Description	Best estimate [uncertainty bounds]	Uncertainty origin	Details	Notes
<i>Dispersal and demographics</i>					
K_d	scale parameter in dispersal kernel	-2.51 [-2.86, -1.82]	drawn from joint 95% confidence limits with θ , weighted by log-likelihood	eqn. 5, SI A.9.0.1, B.2	estimated in Cata-lano et al. (in prep) using methods in Bode et al. (2018)
θ	shape parameter in dispersal kernel	1.49 [0.87, 2.46]	drawn from joint 95% confidence limits with K_d , weighted by log-likelihood	eqn. 5, SI A.9.0.1, B.2	estimated in Cata-lano et al. (in prep) using methods in Bode et al. (2018)
L_∞	average asymptotic size (cm) in von Bertalanffy growth curve	10.7 cm [9.8, 11.6]	growth curve estimated with different pairs of fish	eqn. 6, SI A.3, A.9.0.2, B.3	
k	growth coefficient in von Bertalanffy growth curve	0.864 [0.795, 0.938]	growth curve estimated with different pairs of fish	eqn. 6, SI A.3, A.9.0.2, B.3	
size _{recruit}	size of a recruit	4.4 cm [3.5-6.0]	sampled from a uniform distribution of range of offspring sizes for parentage analyses	SI A.1, A.9.0.5	used as starting size of fish in calculation of LEP (eqn. 7)

b	intercept at 0 cm for size-fecundity relationship	1.174 eggs	no uncertainty	eqn. A.1, SI A.4	
β_l	size effect for size-fecundity relationship	2.388 $\frac{\text{eggs}}{\text{cm}}$	no uncertainty	eqn. A.1, SI A.4	
β_e	egg age effect in fecundity	-0.608	no uncertainty	eqn. A.1, SI A.4	egg age was determined by the presence of visible eyes (eyed vs. non-eyed)
c_e	number of egg clutches per year	11.9	no uncertainty	eqn. A.1, SI A.4	estimate from Holtswarth et al. (2017)
size_{sd}	spread in sizes of fish one year later	1.45	no uncertainty	used in estimating LEP, SI A.5	estimated from recapture data
parent size	size of fish used to estimate LEP for parents (LEPp)	6.0 cm	no uncertainty	SI A.5	used in estimating egg-recruit survival (S_e , eqn. 8)
R_m	number of offspring matched to genotyped parents	71 [55, 87]	random binomial for each genotyped offspring using the assignment rate from the parentage analysis (9%)	SI A.9.0.8	used in calculating egg-recruit survival (S_e , eqn. 8)

ξ

genotyped offspring	number of recruits genotyped	791	no uncertainty	SI B.1	used to find mean recruit size ($\text{size}_{\text{recruit}}$), estimate metrics with immigrants included
N_g	potential parents genotyped	1729	no uncertainty	SI B.1	used to find proportion of dispersal kernel area sampled (P_d , SI A.8)
L_f	size of transition to female	9.3 cm [5.2, 12.7]	sampled with replacement from transition sizes for recaptured fish	eqn. A.1, SI A.9.0.4	used to find fecundity (eqn. A.1)
$b_{\phi,ES}$	intercept at size = 0cm for survival at Elementary School patch	-1.88 [-3.33, -0.44]	sampled from within 95% confidence limits from MARK estimates	eqn. B.1, SI A.3, A.9.0.3, B.4	patch with median survival
b_a	size effect for survival	0.15 [0.10, 0.21]	sampled from within 95% confidence limits from MARK estimates	eqn. B.1, SI A.3, A.9.0.3, B.4	

Scaling factors

DD	proportional increase in unoccupied anemones to account for density-dependence at settlement	1.18	no uncertainty	section "Accounting for density-dependence", SI A.6	used to scale recruits for egg-recruit survival (S_e , eqn. 8)
p_A	proportion anemones occupied by yellow-tail anemonefish	0.37	no uncertainty	SI A.6	
p_U	proportion anemones unoccupied by anemonefish	0.46	no uncertainty	SI A.6	
P_h	cumulative proportion of habitat in patches sampled	0.41	no uncertainty	SI A.8.0.1	used to scale recruits for egg-recruit survival (S_e , eqn. 8)
P_s	proportion of region that was habitat	0.20	no uncertainty	SI A.8.0.4	used to scale recruits for egg-recruit survival (S_e , eqn. 8)
P_d	proportion dispersal kernel area in sampling region	0.57	no uncertainty	SI A.8.0.3	used to scale recruits for egg-recruit survival (S_e , eqn. 8)
P_c	probability of capturing a fish	0.56	sampled from a beta distribution	SI A.8.0.2, A.9.0.6	used to scale recruits for egg-recruit survival (S_e , eqn. 8)

Table A2: Table with patch-specific survival (ϕ_i) values on a log-odds scale (used in eqn. B.1), where the intercept is for adult survival for a fish of size 0 cm. The intercept for each patch is the intercept for Cabatoan plus the additional intercept value for that patch, shown in the table.

Patch	Intercept	Standard error	Confidence limits	Notes
Cabatoan	-1.78	0.33	-2.42 to -1.14	
Caridad Cemetery	-19.66	0.00	-19.66 to -19.66	addition to Cabatoan intercept
Elementary School	-0.11	0.41	-0.92 to 0.69	addition to Cabatoan intercept
Gabas	-0.42	0.58	-1.55 to 0.72	addition to Cabatoan intercept
Haina	0.12	0.35	-0.57 to 0.81	addition to Cabatoan intercept
Higcop South	-0.06	0.46	-0.96 to 0.84	addition to Cabatoan intercept
N. Magbangon	-1.31	0.38	-2.05 to -0.57	addition to Cabatoan intercept
Palanas	0.24	0.26	-0.26 to 0.75	addition to Cabatoan intercept
Poroc Rose	-0.19	0.44	-1.05 to 0.68	addition to Cabatoan intercept
Poroc San Flower	-0.52	0.48	-1.45 to 0.42	addition to Cabatoan intercept
San Agustin	-0.47	0.50	-1.45 to 0.42	addition to Cabatoan intercept
Sitio Baybayon	0.02	0.26	-0.49 to 0.52	addition to Cabatoan intercept
S. Magbangon	-1.08	0.48	-2.02 to -0.14	addition to Cabatoan intercept
Tomakin Dako	0.39	0.33	-0.25 to 1.03	addition to Cabatoan intercept
Visca	0.33	0.35	-0.36 to 1.01	addition to Cabatoan intercept
Wangag	0.35	0.25	-0.15 to 0.85	addition to Cabatoan intercept

Table A3: Table showing the set of models considered in MARK for survival (ϕ , from eqn. B.1) and recapture probability (p_r , from eqn. B.2), including effects of fish size (L), minimum distance from diver to the anemone where the fish was first caught during surveys (D), year (t), and patch (i), and their relative AICc scores.

Model	Model description	AICc	dAICc
$\phi \sim L + i, p_r \sim L + D$	survival size+patch, recapture size+distance	3104.1	0
$\phi \sim i, p_r \sim L + D$	survival patch, recapture size+distance	3127.2	-23.1
$\phi \sim i, p_r \sim D$	survival patch, recapture distance	3127.2	-23.1
$\phi \sim L, p_r \sim L + D$	survival size, recapture size+distance	3139.9	-35.8
$\phi \sim L, p_r \sim D$	survival size, recapture distance	3141.6	-37.5
$\phi, p_r \sim L + D$	survival constant, recapture size+distance	3168.4	-64.3
$\phi, p_r \sim D$	survival constant, recapture distance	3169.3	-65.2
$\phi \sim t, p_r$	survival time, recapture constant	3243.9	-139.8
$\phi \sim i, p_r$	survival patch, recapture constant	3254.4	-150.3
$\phi, p_r \sim t$	survival constant, recapture time	3274.0	-169.9
$\phi \sim L, p_r \sim L$	survival size, recapture size	3345.1	-241.0
ϕ, p_r	survival constant, recapture constant	3382.7	-278.6

Table A4: Table showing the percent of anemones surveyed at each patch, ordered from north to south, in each sampling year.

		% Habitat surveyed						
Patch	# Total anems	2012	2013	2014	2015	2016	2017	2018
Palanas	138	29	57	48	61	85	86	86
Wangag	291	18	33	42	35	27	49	69
N. Magbangon	105	5	12	40	63	64	0	5
S. Magbangon	34	41	56	32	0	65	0	71
Cabatoan	26	42	58	58	65	73	0	62
Caridad Cemetery	4	0	75	50	0	50	50	50
Caridad Proper	4	0	100	0	0	0	0	0
Hicgop South	18	0	67	28	28	56	83	78
Sitio Tugas	8	0	100	0	0	0	0	0
Elementary School	7	0	100	43	100	100	86	100
Sitio Lonas	1	100	100	0	0	0	0	0
San Agustin	18	89	61	72	61	100	89	72
Poroc San Flower	11	100	82	73	73	55	82	64
Poroc Rose	13	100	100	69	31	23	69	69
Visca	13	100	100	23	38	62	85	62
Gabas	9	0	0	0	44	44	67	0
Tomakin Dako	48	0	25	23	38	35	60	69
Haina	104	0	6	13	13	10	56	80
Sitio Baybayon	259	0	14	30	34	30	41	81
Overall	1111	16	32	36	39	42	48	67

Table A5: Table showing patch-specific estimates of lifetime egg production (LEP_i), lifetime recruit production (LRP_i), and self persistence (SP_i)

Patch	LEP_i	LRP_i	SP_i
Palanas	1383	2.91	0.017
Wangag	1642	3.45	0.040
N. Magbangon	133	0.28	0.002
S. Magbangon	183	0.39	0.003
Cabatoan	933	1.96	0.009
Caridad Cemetery	0	0	0
Caridad Proper	781	1.64	0.004
Hicop South	848	1.78	0.017
Sitio Tugas	781	1.64	0.003
Elementary School	781	1.64	0.007
Sitio Lonas	781	1.64	0
San Agustin	445	0.92	0.006
Poroc San Flower	415	0.87	0.002
Poroc Rose	694	1.46	0.014
Visca	1586	3.34	0.021
Gabas	483	1.02	0.003
Tomakin Dako	1760	3.70	0.022
Haina	1130	2.38	0.044
Sitio Baybayon	959	2.02	0.021

D Supplemental Figures

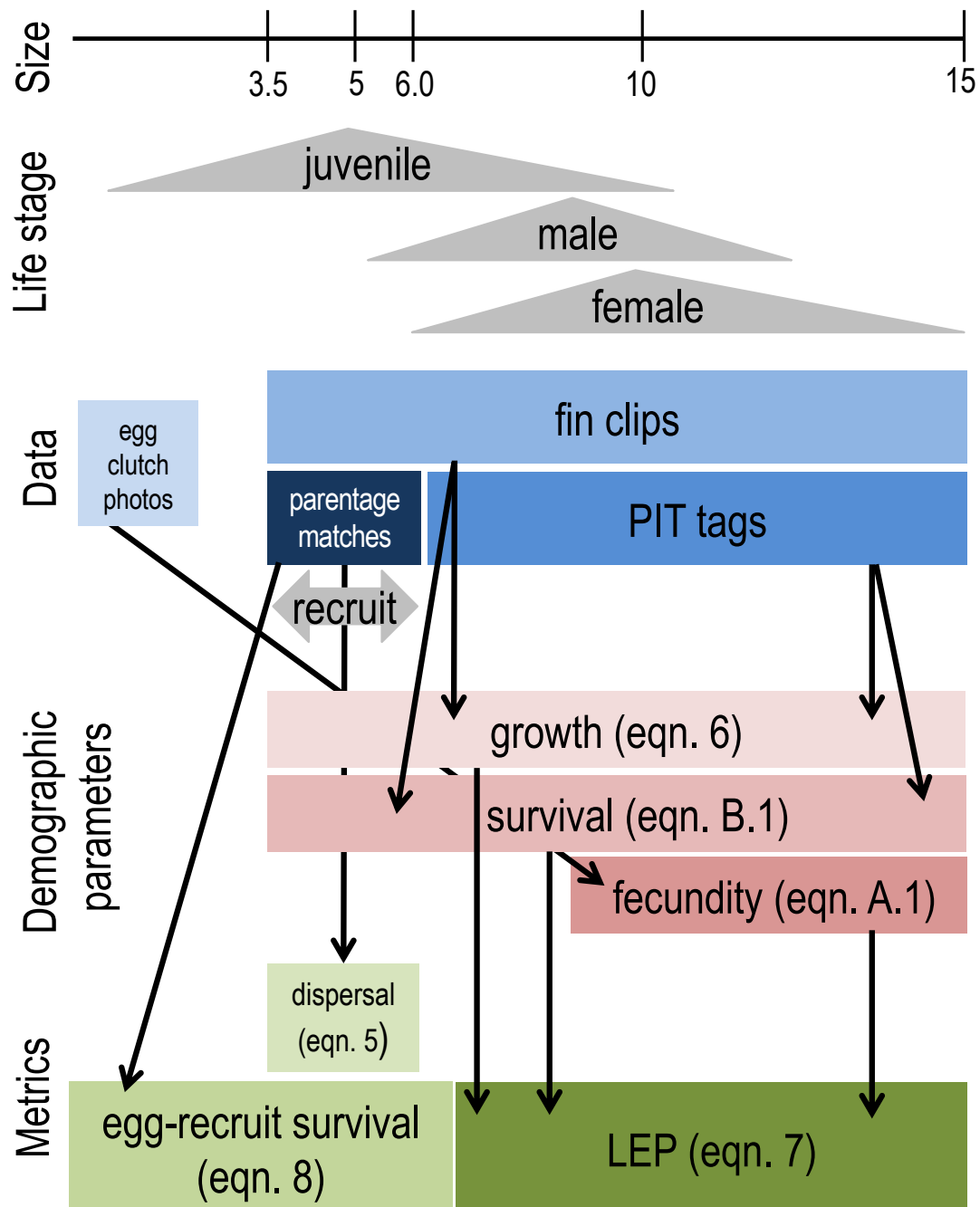


Figure D.1: The data collected for fish at each life stage and how they match to the equations and metrics estimated. We considered recruits to be offspring in their first year of settlement, represented by the 3.5–6.0 cm range (SI A.1).

How could we have missed potential recruits originating from our patches?

- 1) Failed to catch recruit when sampling (P_c)
- 2) Missed sampling some habitat areas within our patches (P_h)
- 3) Recruit dispersed outside our study region (P_d)
- 4) Recruit dispersed to non-habitat within our region (P_s)
- 5) Recruit died due to density-dependent competition with other settlers (DD)

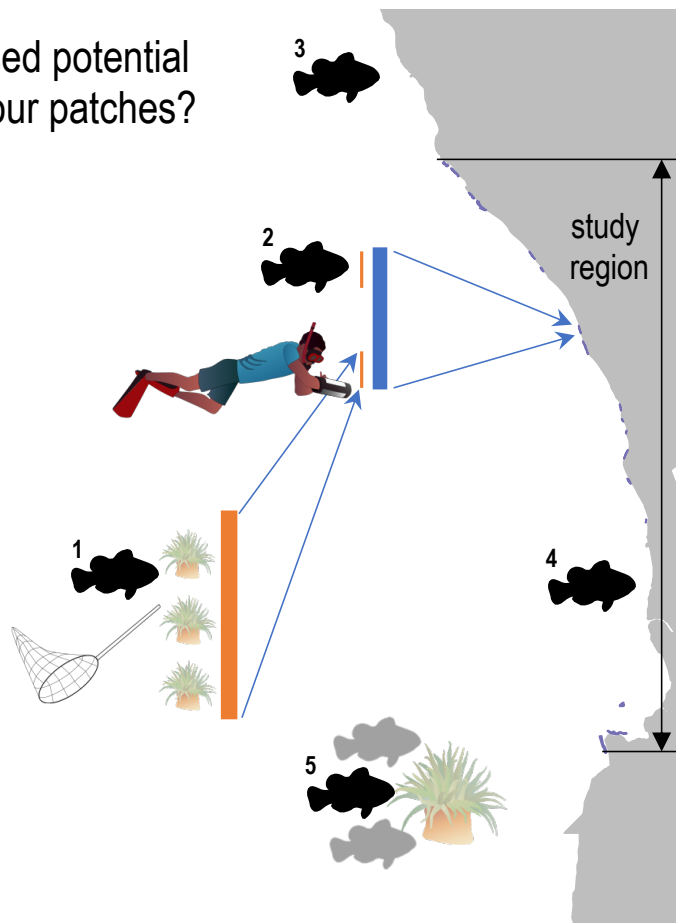


Figure D.2: Schematic of five ways we could have missed recruits while sampling. We used these factors to scale up our raw estimate of recruits from matched offspring (SI A.8).

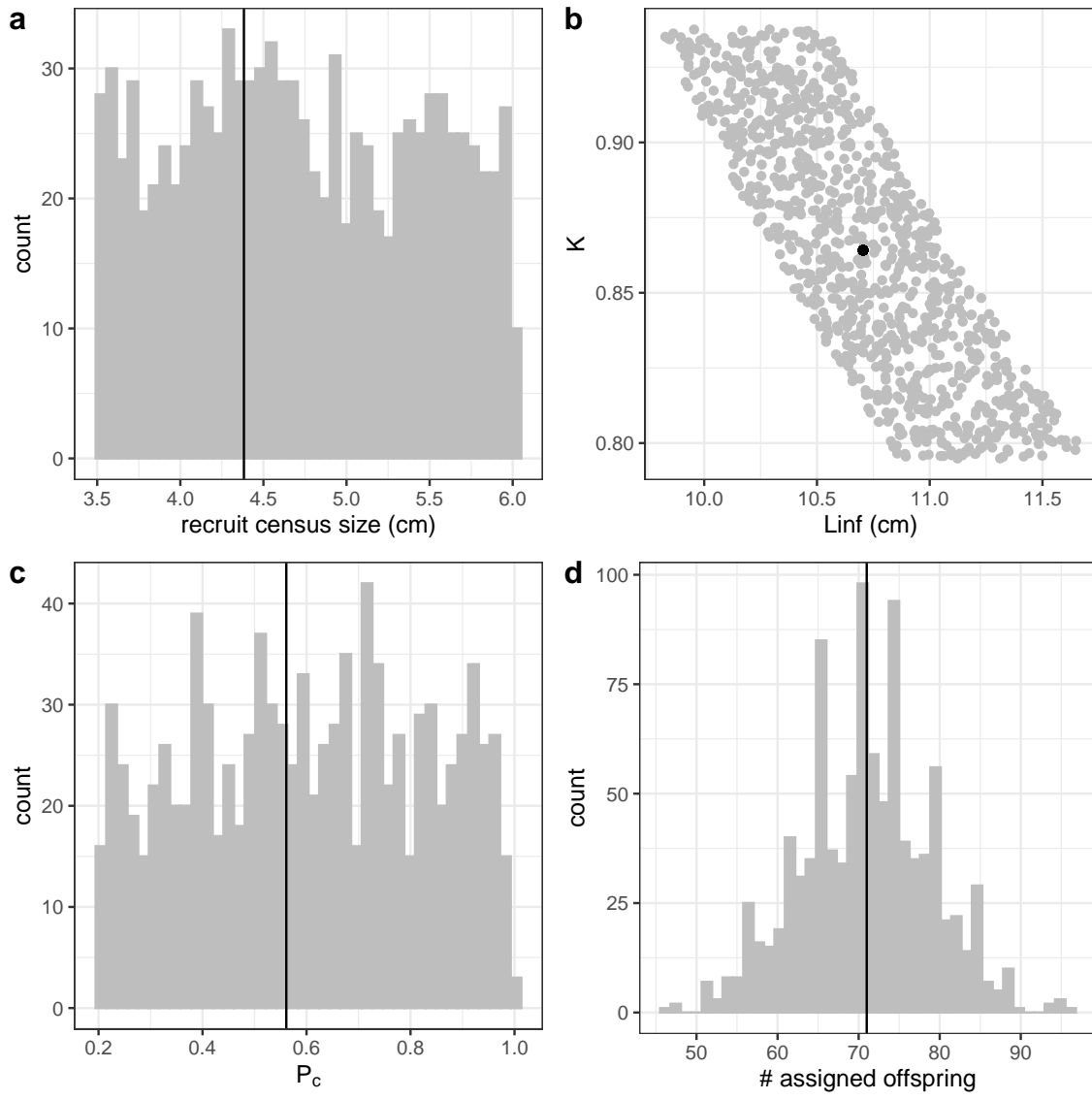


Figure D.3: Range of parameter inputs for uncertainty runs with all uncertainty included, where the black line or point is the value used for the best estimate: a) $\text{size}_{\text{recruit}}$, the census size for recruits after egg-recruit survival; b) the parameters L_{∞} and k of the von Bertalanffy growth model; c) P_c , the probability of capturing a fish; d) number of offspring assigned back to parents in the parentage analysis.

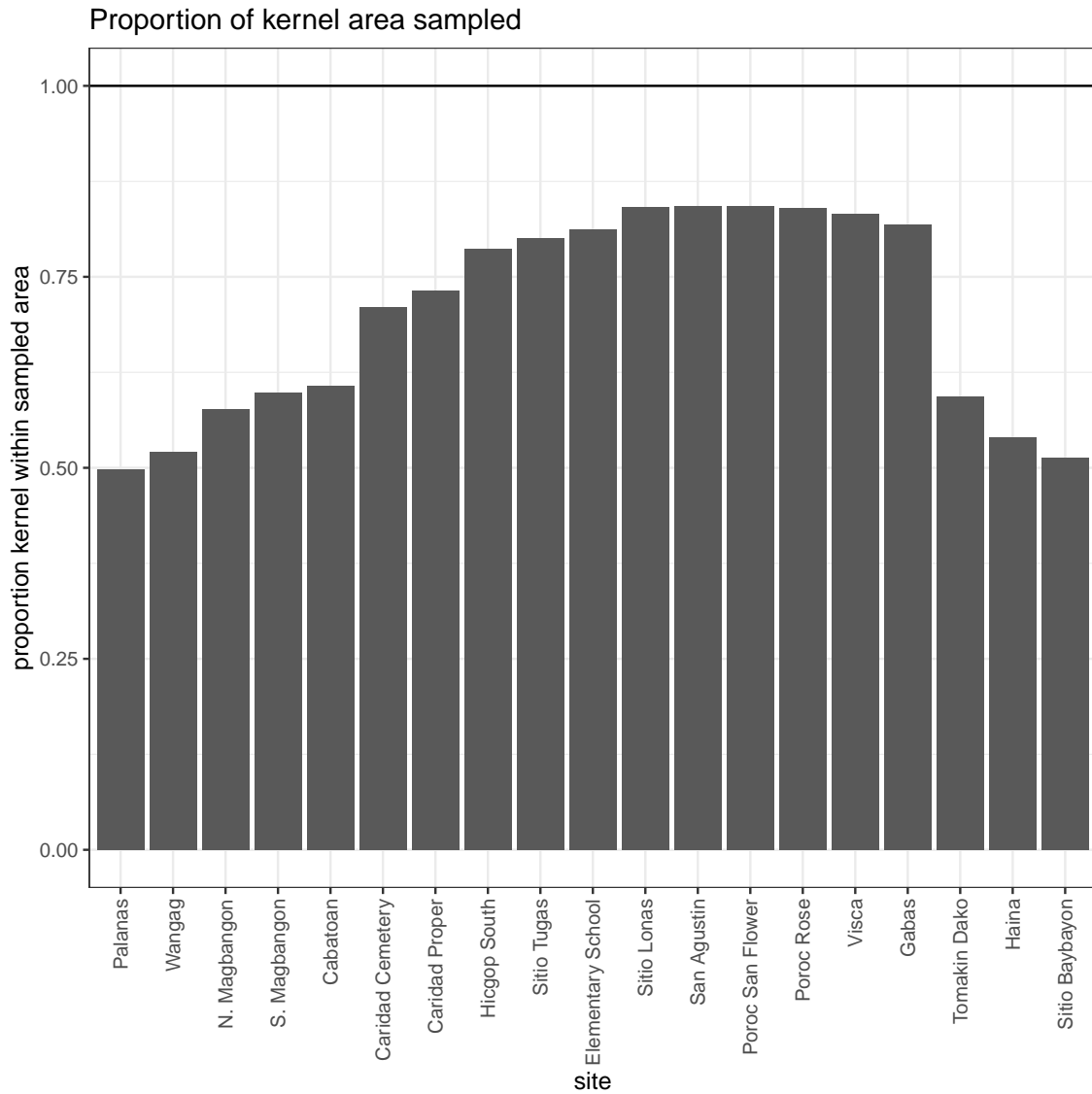


Figure D.4: Proportion of the dispersal kernel area from the center of each patch covered by our sampling region ($\frac{A_i}{N_{g,i}}$ from eqn. A.3). The overall proportion (P_d) is weighted by the number of parents at each patch.

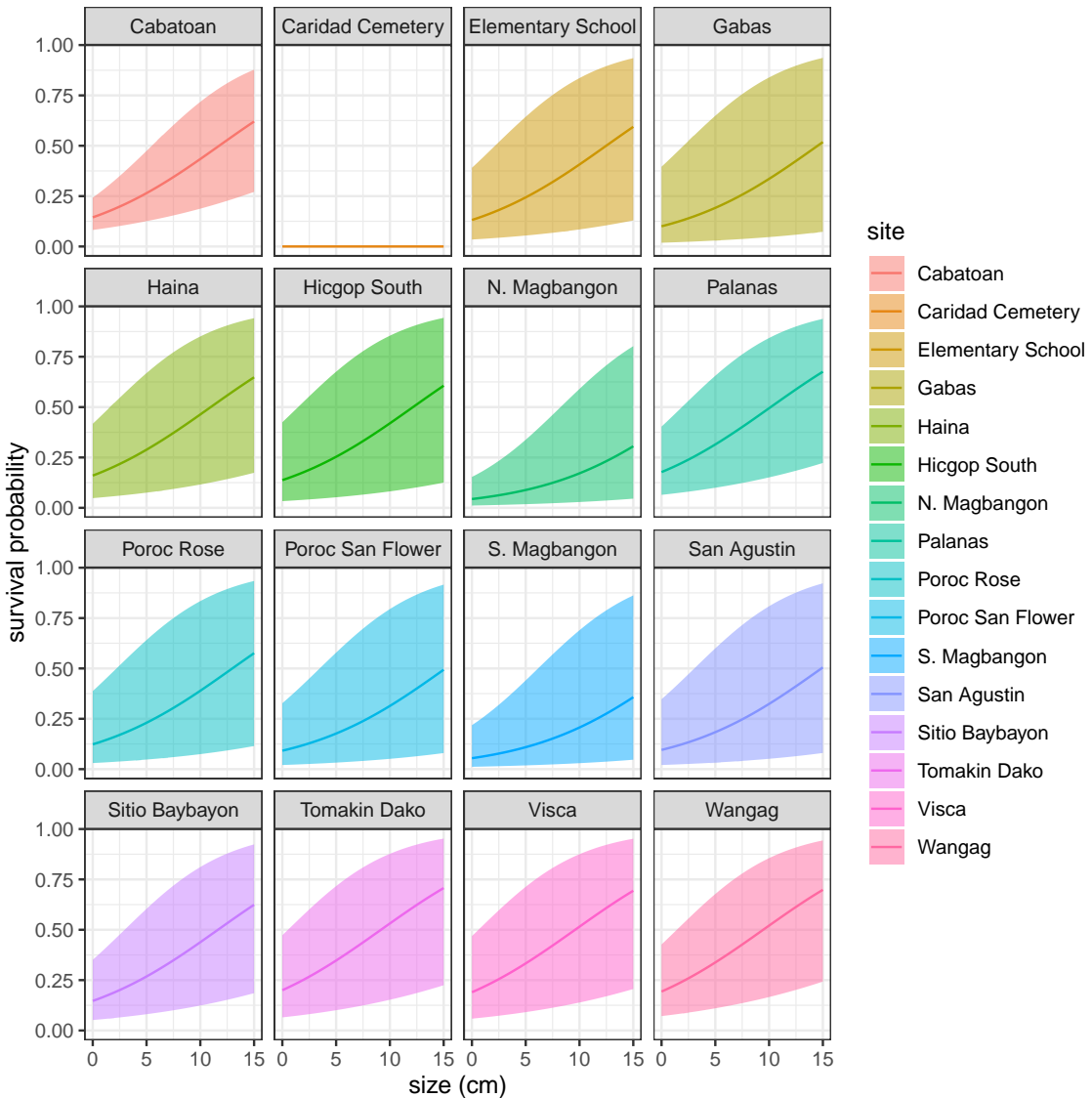


Figure D.5: Annual survival (ϕ) by fish size at each patch, detailed in SI A.3, A.9.0.3, and B.4.

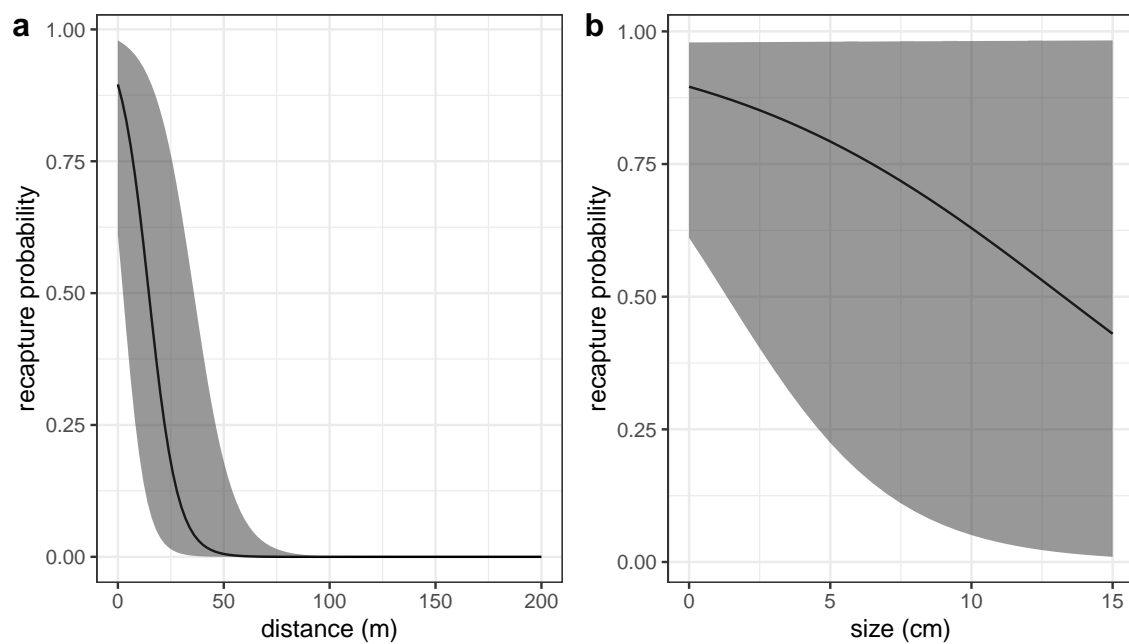


Figure D.6: Effects of a) minimum distance between divers and the anemone where the fish was first caught and b) fish size on recapture probability, estimated along with survival in a mark-recapture analysis (SI A.3, B.4).

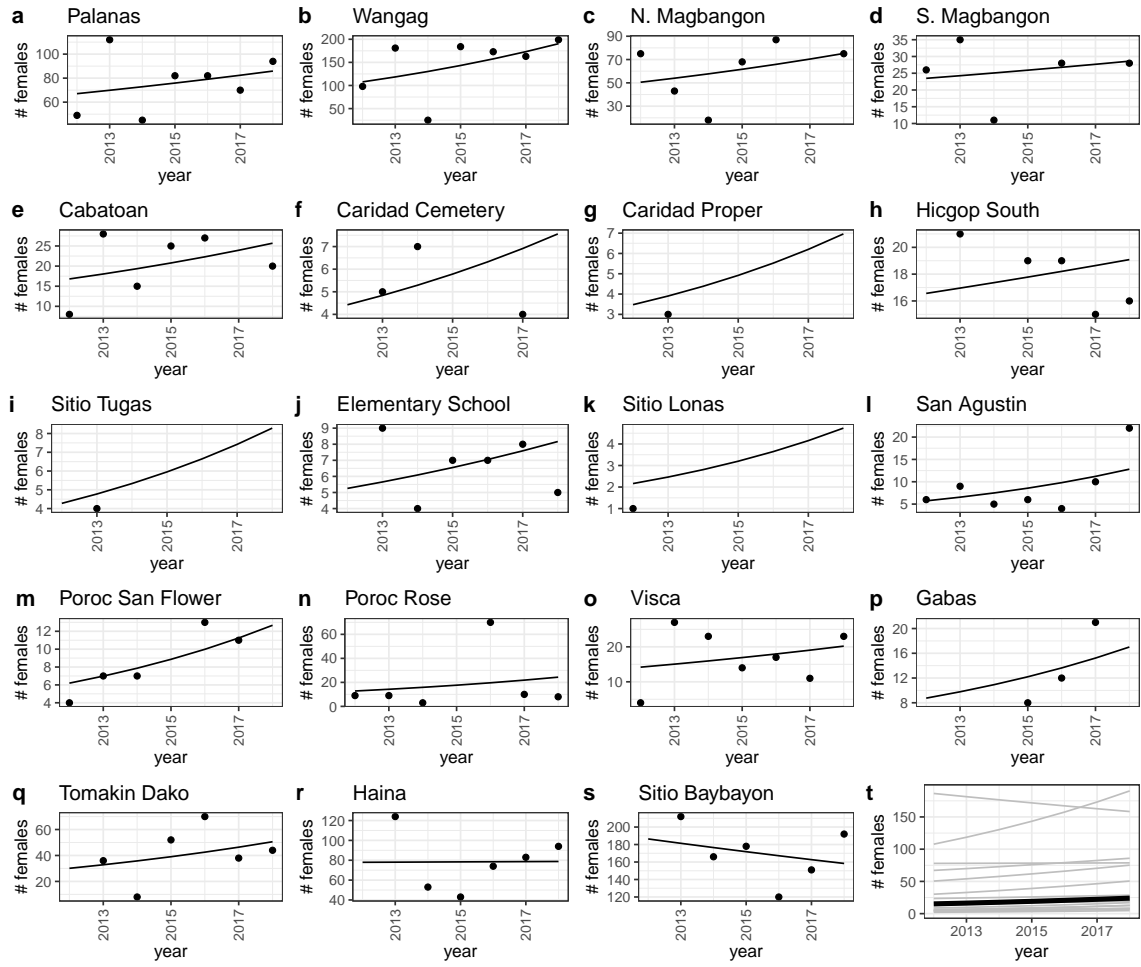


Figure D.7: Scaled number of females captured (black dots) and abundance trends (black lines) by patch from a mixed effects model with patch as a random effect.

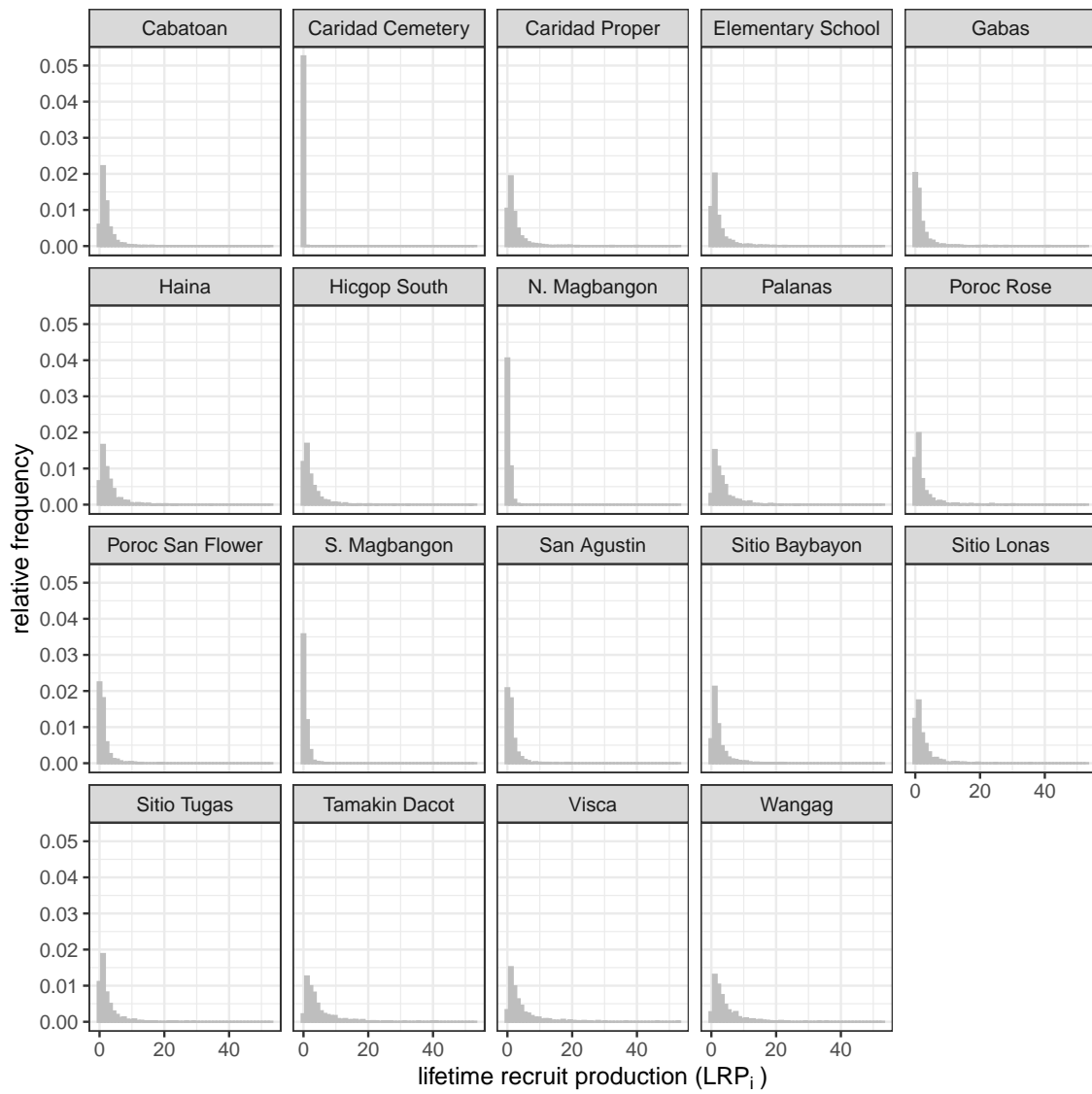


Figure D.8: Patch-specific lifetime recruit production (LRP_i) estimates.

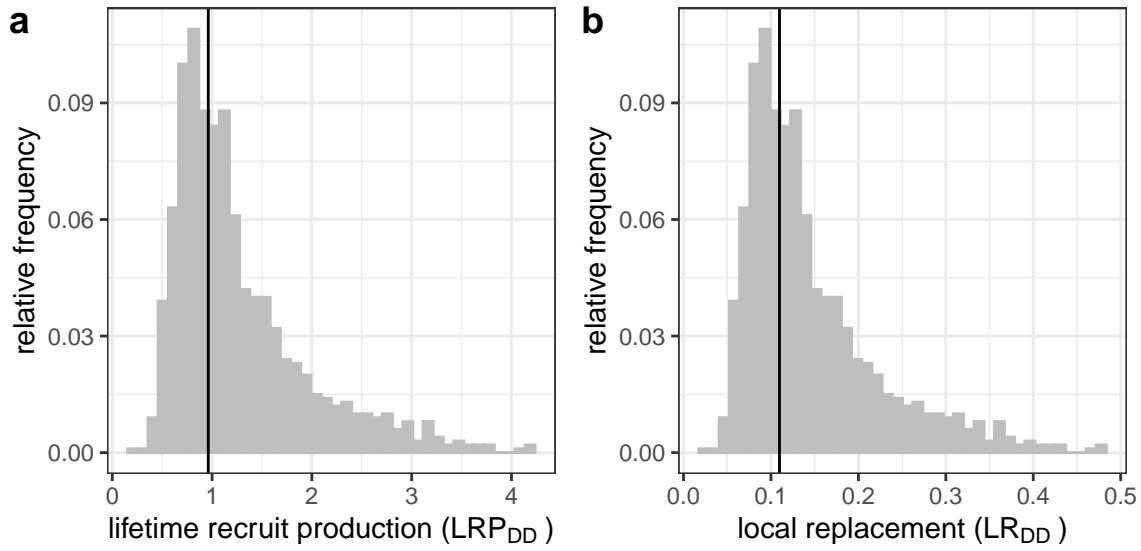


Figure D.9: Estimates of a) LRP averaged across patches, and b) local replacement without compensating for density dependence in early life stages in our data, showing the best estimate (black solid line) and range of estimates considering uncertainty (grey). These estimates compare to those in Fig. 4b and c, where we corrected for additional mortality in early life due to density dependence.

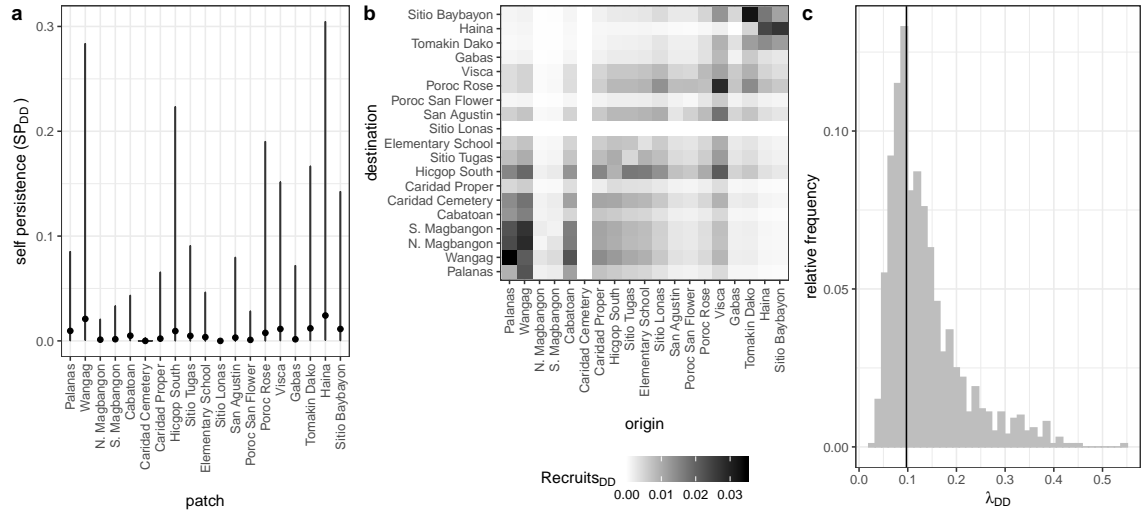


Figure D.10: Values of a) self-persistence (SP_{DD}), b) realized connectivity among patches ($C_{i,j,DD}$), and c) network persistence ($\lambda_{c,DD}$) without compensation for density-dependence in early life stages in our data. For self-persistence (a) and network persistence (c), the best estimate is shown with in black (point for (a), line for (c)) and the range of estimates considering uncertainty is shown in grey. These estimates compare to those in Fig. 5 where we compensated for density dependence in early life stages.

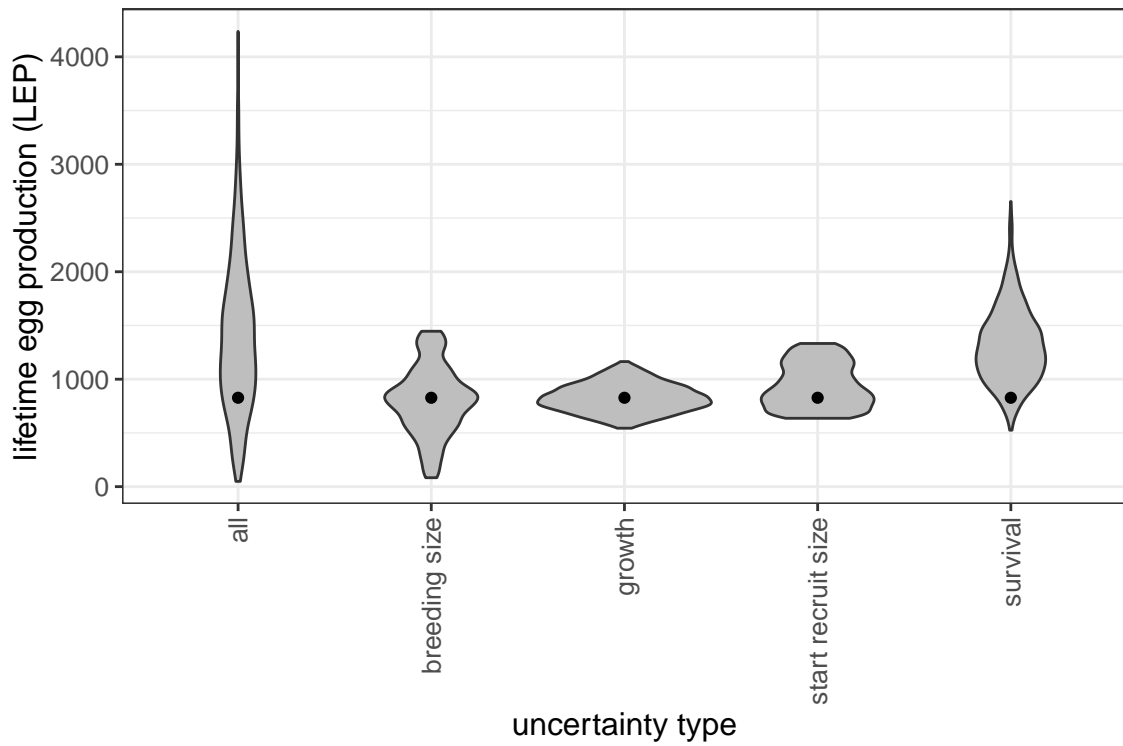


Figure D.11: The contribution of different sources of uncertainty in LEP averaged across patches (LEP_*). We calculated the metrics using best estimates for all inputs except the one shown and show the results as violin plots, which show vertical probability densities of the metrics across a range of values.

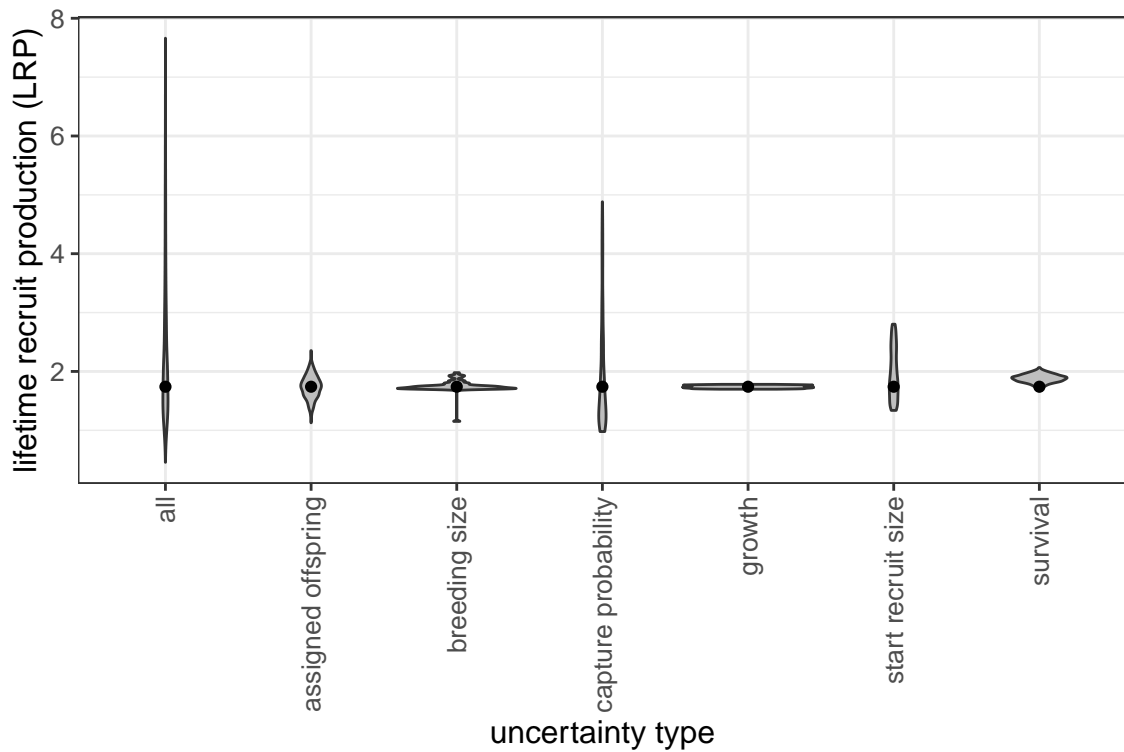


Figure D.12: The contribution of different sources of uncertainty in LRP. We calculated the metrics using best estimates for all inputs except the one shown and show the results as violin plots, which show vertical probability densities of the metrics across a range of values.

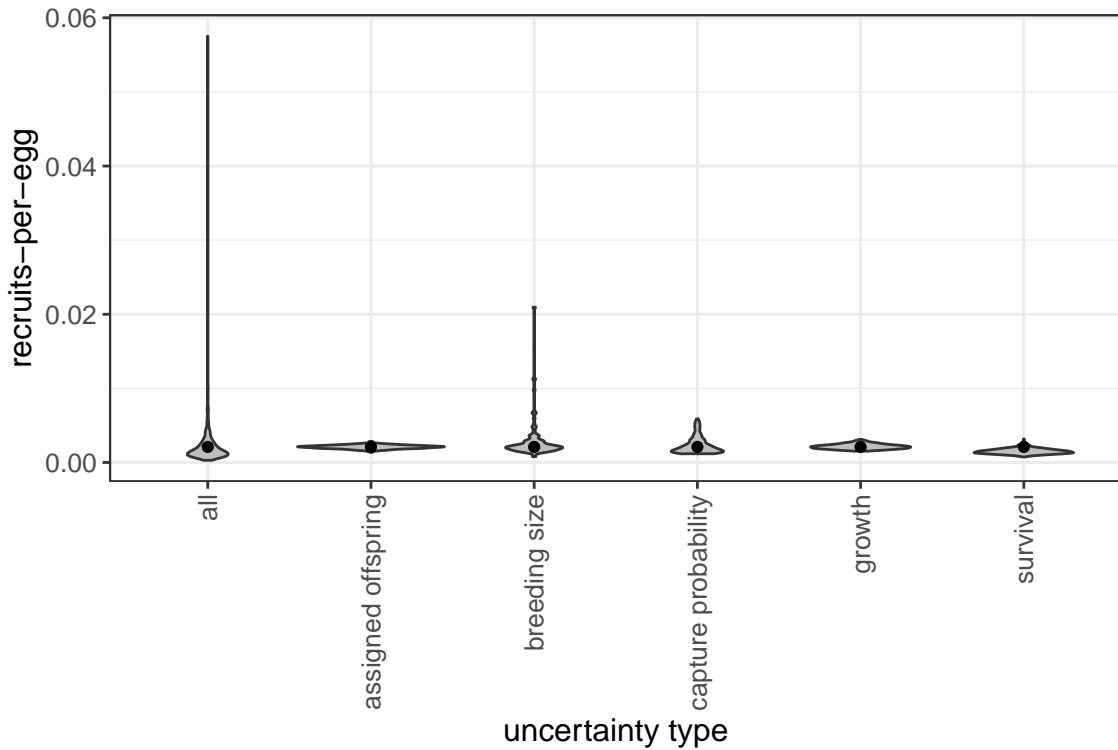


Figure D.13: The contribution of different sources of uncertainty in egg-recruit survival (S_e). We calculated the metrics using best estimates for all inputs except the one shown and show the results as violin plots, which show vertical probability densities of the metrics across a range of values.

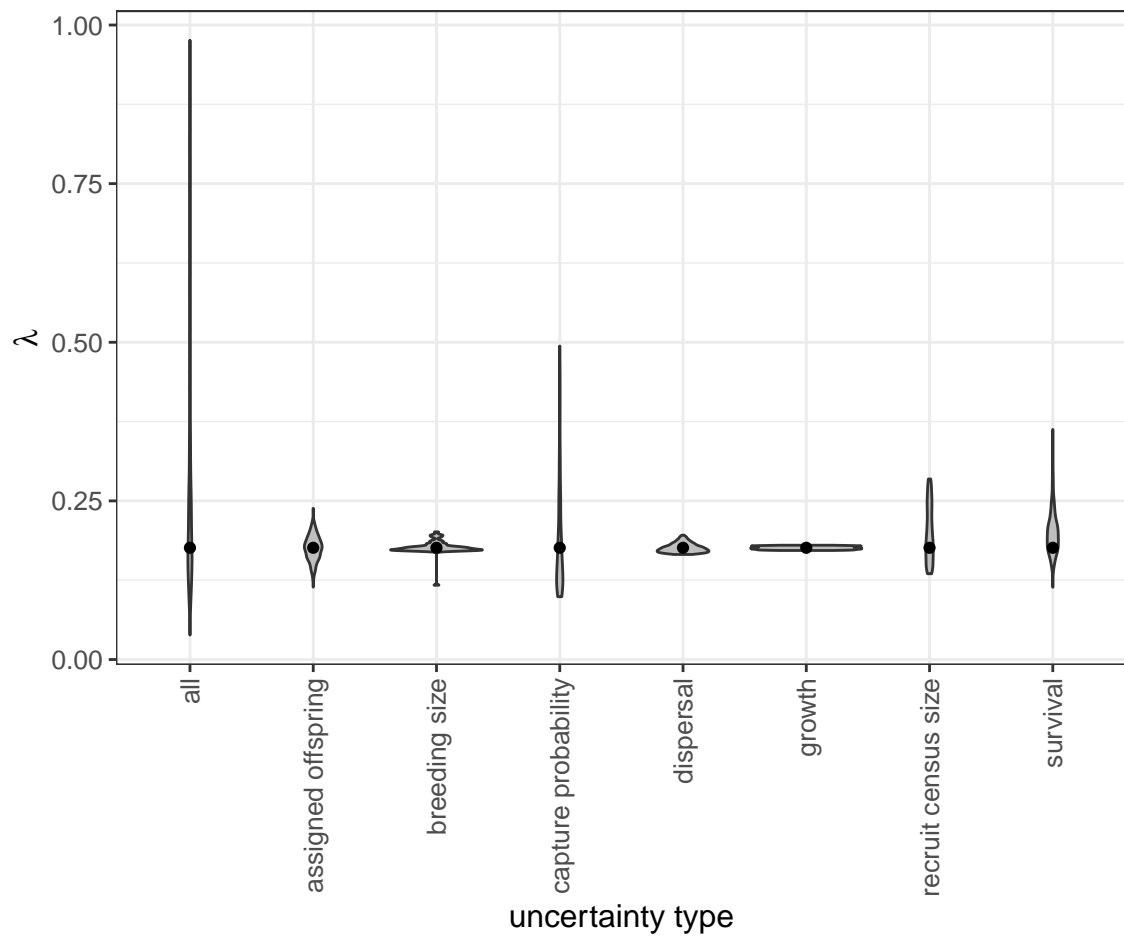


Figure D.14: The contribution of different sources of uncertainty in network persistence (λ_c). We calculated the metrics using best estimates for all inputs except the one shown and show the results as violin plots, which show vertical probability densities of the metrics across a range of values.

⁷⁶² References

- Glenn R Almany, Serge Planes, Simon R Thorrold, Michael L Berumen, Michael Bode, Pablo Saenz-Agudelo, Mary C Bonin, Ashley J Frisch, Hugo B Harrison,
⁷⁶⁵ Vanessa Messmer, et al. Larval fish dispersal in a coral-reef seascape. *Nature Ecology & Evolution*, 1:0148, 2017.
- Michael Arvedlund, Mark I McCormick, Daphne G Fautin, and Mogens Bildsøe. Host
⁷⁶⁸ recognition and possible imprinting in the anemonefish *amphiprion melanopus* (pisces: Pomacentridae). *Marine Ecology Progress Series*, 188:207–218, 1999.
- Diana S Baetscher, Eric C Anderson, Elizabeth A Gilbert-Horvath, Daniel P Malone,
⁷⁷¹ Emily T Saarman, Mark H Carr, and John Carlos Garza. Dispersal of a nearshore marine fish connects marine reserves and adjacent fished areas along an open coast. *Molecular ecology*, 28(7):1611–1623, 2019.
- ⁷⁷⁴ Douglas Bates, Martin Mächler, Ben Bolker, and Steve Walker. Fitting linear mixed-effects models using lme4. *Journal of Statistical Software*, 67(1):1–48, 2015. doi: 10.18637/jss.v067.i01.
- ⁷⁷⁷ David R Bellwood and Rebecca Fisher. Relative swimming speeds in reef fish larvae. *Marine Ecology Progress Series*, 211:299–303, 2001.
- Michael Bode, David H Williamson, Hugo B Harrison, Nick Outram, and Geoffrey P
⁷⁸⁰ Jones. Estimating dispersal kernels using genetic parentage data. *Methods in Ecology and Evolution*, 9(3):490–501, 2018.

- Michael Bode, Jeffrey M. Leis, Luciano B. Mason, David H. Williamson, Hugo B.
783 Harrison, Severine Choukroun, and Geoffrey P. Jones. Successful validation of a
larval dispersal model using genetic parentage data. *PLOS Biology*, 17(7):1–13,
07 2019. doi: 10.1371/journal.pbio.3000380. URL <https://doi.org/10.1371/journal.pbio.3000380>.
- Louis W. Botsford, Alan Hastings, and Steven D. Gaines. Dependence of sustainability on the configuration of marine reserves and larval dispersal distance. *Ecology Letters*, 4:144–150, 2001.
789
- Louis W Botsford, J Wilson White, and Alan Hastings. *Population Dynamics for Conservation*. Oxford University Press, 2019.
- 792 Scott C Burgess, Kerry J Nickols, Chris D Griesemer, Lewis AK Barnett, Allison G Dedrick, Erin V Satterthwaite, Lauren Yamane, Steven G Morgan, J Wilson White, and Louis W Botsford. Beyond connectivity: how empirical methods can quantify population persistence to improve marine protected-area design. *Ecological Applications*, 24(2):257–270, 2014.
- Peter Buston. Forcible eviction and prevention of recruitment in the clown anemonefish. *Behavioral Ecology*, 14(4):576–582, 2003a.
798
- Peter Buston. Social hierarchies: size and growth modification in clownfish. *Nature*, 424(6945):145–146, 2003b.
- 801 Peter M Buston and Cassidy C DAloia. Marine ecology: reaping the benefits of local dispersal. *Current Biology*, 23(9):R351–R353, 2013.

- Peter M Buston and Jane Elith. Determinants of reproductive success in dominant
804 pairs of clownfish: a boosted regression tree analysis. *Journal of Animal Ecology*,
80(3):528–538, 2011.
- Peter M Buston, Geoffrey P Jones, Serge Planes, and Simon R Thorrold. Probability
807 of successful larval dispersal declines fivefold over 1 km in a coral reef fish. *Proceedings of the Royal Society of London B: Biological Sciences*, page rspb20112041,
2011.
- Henry S Carson, Geoffrey S Cook, Paola C López-Duarte, and Lisa A Levin. Evaluating
810 the importance of demographic connectivity in a marine metapopulation. *Ecology*, 92(10):1972–1984, 2011.
- Katrina A Catalano, Allison G Dedrick, Michelle Stuart, Jonathan Purtiz, Humberto
813 Montes, Jr., and Malin Pinsky. Interannual variability of genetic connectivity in
a coral reef fish *Amphiprion clarkii*. in prep.
- Joshua E Cinner, Cindy Huchery, M Aaron MacNeil, Nicholas AJ Graham, Tim R
816 McClanahan, Joseph Maina, Eva Maire, John N Kittinger, Christina C Hicks,
Camilo Mora, et al. Bright spots among the worlds coral reefs. *Nature*, 535(7612):
819 416–419, 2016.
- MA Coleman, P Cetina-Heredia, M Roughan, M Feng, E van Sebille, and BP Ke-
laher. Anticipating changes to future connectivity within a network of marine
822 protected areas. *Global Change Biology*, 2017.

- C. C. D'Aloia, S. M. Bogdanowicz, J. E. Majoris, R. G. Harrison, and P. M. Buston.
Self-recruitment in a Caribbean reef fish: a method for approximating dispersal
kernels accounting for seascape. *Molecular Ecology*, 22(9):2563–2572, May 2013.
ISSN 09621083. doi: 10.1111/mec.12274. URL <http://doi.wiley.com/10.1111/mec.12274>.
- JK Elliott, JM Elliott, and RN Mariscal. Host selection, location, and association
behaviors of anemonefishes in field settlement experiments. *Marine Biology*, 122
(3):377–389, 1995.
- Stephen P Ellner, Dylan Z Childs, Mark Rees, et al. Data-driven modelling of
structured populations. *A practical guide to the Integral Projection Model*. Cham:
Springer, 2016.
- Lenore Fahrig. How much habitat is enough? *Biological conservation*, 100(1):65–74,
2001.
- Daphne Gail Fautin, Gerald R Allen, Gerald Robert Allen, Australia Naturalist,
Gerald Robert Allen, and Australie Naturaliste. Field guide to anemonefishes and
their host sea anemones. 1992.
- Will F Figueira. Connectivity or demography: defining sources and sinks in coral
reef fish metapopulations. *Ecological Modelling*, 220(8):1126–1137, 2009.
- Will F Figueira and Larry B Crowder. Defining patch contribution in source-sink
metapopulations: the importance of including dispersal and its relevance to marine
systems. *Population Ecology*, 48(3):215–224, 2006.

- Will F Figueira, Sean J Lyman, Larry B Crowder, and Gil Rilov. Small-scale demographic variability of the bicolor damselfish, *stegastes partitus*, in the florida keys usa. *Environmental Biology of Fishes*, 81(3):297–311, 2008.
- Rebecca Fisher. Swimming speeds of larval coral reef fishes: impacts on self-recruitment and dispersal. *Marine Ecology Progress Series*, 285:223–232, 2005.
- Emma Fuller, Eleanor Brush, and Malin L Pinsky. The persistence of populations facing climate shifts and harvest. *Ecosphere*, 6(9):1–16, 2015.
- Lysel Garavelli, J Wilson White, Iliana Chollett, and Laurent Marcel Chérubin. Population models reveal unexpected patterns of local persistence despite widespread larval dispersal in a highly exploited species. *Conservation Letters*, 11(5):e12567, 2018.
- Sarah O Hameed, J Wilson White, Seth H Miller, Kerry J Nickols, and Steven G Morgan. Inverse approach to estimating larval dispersal reveals limited population connectivity along 700 km of wave-swept open coast. *Proceedings of the Royal Society B: Biological Sciences*, 283(1833):20160370, 2016.
- Ilkka Hanski. Metapopulation dynamics. *Nature*, 396(6706):41–49, 1998.
- Kyle E Harms, S Joseph Wright, Osvaldo Calderón, Andres Hernandez, and Edward Allen Herre. Pervasive density-dependent recruitment enhances seedling diversity in a tropical forest. *Nature*, 404(6777):493–495, 2000.
- Deborah R Hart and Antonie S Chute. Estimating von bertalanffy growth parameters

- 864 from growth increment data using a linear mixed-effects model, with an application
to the sea scallop *placopecten magellanicus*. *ICES Journal of Marine Science*, 66
(10):2165–2175, 2009.
- 867 Alan Hastings and Louis W. Botsford. Persistence of spatial populations depends on
returning home. *Proceedings of the National Academy of Sciences*, 103:6067–6072,
2006.
- 870 Akihisa Hattori and Yasunobu Yanagisawa. Life-history pathways in relation to
gonadal sex differentiation in the anemonefish, *amphiprion clarkii*, in temperate
waters of japan. *Environmental Biology of Fishes*, 31(2):139–155, 1991.
- 873 Kina Hayashi, Katsunori Tachihara, and James Davis Reimer. Low density popu-
lations of anemonefish with low replenishment rates on a reef edge with anthro-
pogenic impacts. *Environmental Biology of Fishes*, 102(1):41–54, 2019.
- 876 Robert J. Hijmans. *geosphere: Spherical Trigonometry*, 2017. URL <https://CRAN.R-project.org/package=geosphere>. R package version 1.5-7.
- Jordan N. Holtswarth, Shem B. San Jose, Humberto R. Montes Jr., James W. Morley,
879 and Malin. L Pinsky. The reproductive seasonality and fecundity of yellowtail
clownfish (*amphiprion clarkii*) off the philippines. *Bulletin of Marine Science*, 93,
2017.
- 882 Darren W Johnson, Mark R Christie, Timothy J Pusack, Christopher D Stallings,
and Mark A Hixon. Integrating larval connectivity with local demography reveals
regional dynamics of a marine metapopulation. *Ecology*, 99(6):1419–1429, 2018.

885 David M. Kaplan, Louis W. Botsford, Michael R. O'Farrell, Steven D. Gaines, and
Salvador Jorgensen. Model-based assessment of persistence in proposed marine
protected area designs. *Ecological Applications*, 19(2):433–448, March 2009. ISSN
888 1051-0761. doi: 10.1890/07-1705.1. URL <http://www.esajournals.org/doi/abs/10.1890/07-1705.1>.

Jacob P Kritzer and Peter F Sale. *Marine metapopulations*. Elsevier Academic Press,
891 2006.

J.L. Laake. RMark: An r interface for analysis of capture-recapture data with
MARK. AFSC Processed Rep. 2013-01, Alaska Fish. Sci. Cent., NOAA,
894 Natl. Mar. Fish. Serv., Seattle, WA, 2013. URL <http://www.afsc.noaa.gov/Publications/ProcRpt/PR2013-01.pdf>.

David Lecchini, Serge Planes, and René Galzin. Experimental assessment of sensory
897 modalities of coral-reef fish larvae in the recognition of their settlement habitat.
Behavioral Ecology and Sociobiology, 58(1):18–26, 2005.

Atte Moilanen, Andrew T Smith, and Ilkka Hanski. Long-term dynamics in a
900 metapopulation of the american pika. *The American Naturalist*, 152(4):530–542,
1998.

Piotr Nowicki and Vladimir Vrabec. Evidence for positive density-dependent emi-
903 gration in butterfly metapopulations. *Oecologia*, 167(3):657, 2011.

Piotr Nowicki, Simona Bonelli, Francesca Barbero, and Emilio Balletto. Relative

importance of density-dependent regulation and environmental stochasticity for
906 butterfly population dynamics. *Oecologia*, 161(2):227–239, 2009.

Haruki Ochi. Mating behavior and sex change of the anemonefish, amphiprion clarkii,
in the temperate waters of southern japan. *Environmental Biology of Fishes*, 26
909 (4):257–275, 1989.

Malin L Pinsky, Humberto R Montes Jr, and Stephen R Palumbi. Using isolation
by distance and effective density to estimate dispersal scales in anemonefish. *Evo-
912 lution*, 64(9):2688–2700, 2010.

BJ Puckett and DB Eggleston. Metapopulation dynamics guide marine reserve de-
sign: importance of connectivity, demographics, and stock enhancement. *Eco-
915 sphere*, 7(6), 2016.

H Ronald Pulliam. Sources, sinks, and population regulation. *The American Natu-
ralist*, 132(5):652–661, 1988.

918 Nicholas L Rodenhouse, T Scott Sillett, Patrick J Doran, and Richard T Holmes.
Multiple density-dependence mechanisms regulate a migratory bird population
during the breeding season. *Proceedings of the Royal Society of London. Series B:
921 Biological Sciences*, 270(1529):2105–2110, 2003.

Océane C Salles, Glenn R Almany, Michael L Berumen, Geoffrey P Jones, Pablo
Saenz-Agudelo, Maya Srinivasan, Simon R Thorrold, Benoit Pujol, and Serge
924 Planes. Strong habitat and weak genetic effects shape the lifetime reproductive
success in a wild clownfish population. *Ecology letters*, 23(2):265–273, 2020.

- Ocane C. Salles, Jeffrey A. Maynard, Marc Joannides, Corentin M. Barbu, Pablo
927 Saenz-Agudelo, Glenn R. Almany, Michael L. Berumen, Simon R. Thorrold, Ge-
offrey P. Jones, and Serge Planes. Coral reef fish populations can persist without
immigration. *Proceedings of the Royal Society B: Biological Sciences*, 282(1819):
930 20151311, November 2015. ISSN 0962-8452, 1471-2954. doi: 10.1098/rspb.2015.
1311. URL <http://rspb.royalsocietypublishing.org/lookup/doi/10.1098/rspb.2015.1311>.
- R Kent Smedbol, Arran McPherson, Michael M Hansen, and Ellen Kenchington.
933 Myths and moderation in marine metapopulations? *Fish and Fisheries*, 3(1):20–
35, 2002.
- James NM Smith and Jessica J Hellmann. Population persistence in fragmented
936 landscapes. *Trends in Ecology & Evolution*, 17(9):397–399, 2002.
- Diane M Thompson, J Kleypas, F Castruccio, Enrique N Curchitser, Malin L Pinsky,
939 B Jönsson, and James R Watson. Variability in oceanographic barriers to coral
larval dispersal: Do currents shape biodiversity? *Progress in oceanography*, 165:
110–122, 2018.
- Nick Tolimieri and Phillip S Levin. The roles of fishing and climate in the population
942 dynamics of bocaccio rockfish. *Ecological Applications*, 15(2):458–468, 2005.
- Mark JA Vermeij and Stuart A Sandin. Density-dependent settlement and mortality
945 structure the earliest life phases of a coral population. *Ecology*, 89(7):1994–2004,
2008.

- Robert R Warner and Peter L Chesson. Coexistence mediated by recruitment fluctuations: a field guide to the storage effect. *The American Naturalist*, 125(6):769–787, 1985.
- Robert R Warner and Terence P Hughes. The population dynamics of reef fishes. 6th International Coral Reef Symposium Executive Committee, 1988.
- J Wilson White and Jameal F Samhouri. Oceanographic coupling across three trophic levels shapes source–sink dynamics in marine metacommunities. *Oikos*, 120(8):1151–1164, 2011.
- J. Wilson White, Mark H Carr, Jennifer E Caselle, Libe Washburn, C. Brock Woodson, Stephen R Palumbi, Peter M Carlson, Robert R Warner, Bruce A Menge, John A Barth, Carol A Blanchette, Peter T Raimondi, and Kristen Milligan. Connectivity, dispersal, and recruitment: Connecting benthic communities and the coastal ocean. *Oceanography*, 32(3):50–59, 2019.
- Jw White, Lw Botsford, A Hastings, and Jl Largier. Population persistence in marine reserve networks: incorporating spatial heterogeneities in larval dispersal. *Marine Ecology Progress Series*, 398:49–67, January 2010. ISSN 0171-8630, 1616-1599. doi: 10.3354/meps08327. URL <http://www.int-res.com/abstracts/meps/v398/p49-67/>.